applied sciences

MDPI

Review

A Review of the Influence of Steel Furnace Slag Type on the Properties of Cementitious Composites

Alexander S. Brand * and Ebenezer O. Fanijo

Charles E. Via, Jr. Department of Civil and Environmental Engineering, Virginia Polytechnic Institute and State University, Blacksburg, VA 24061, USA; ebenfanijo@vt.edu

* Correspondence: asbrand@vt.edu

Received: 18 October 2020; Accepted: 17 November 2020; Published: 19 November 2020

Abstract: The type of steel furnace slag (SFS), including electric arc furnace (EAF) slag, basic oxygen furnace (BOF) slag, ladle metallurgy furnace (LMF) slag, and argon oxygen decarburization (AOD) slag, can significantly affect the composite properties when used as an aggregate or as a supplementary cementitious material in bound applications, such as concretes, mortars, alkali-activated materials, and stabilized soils. This review seeks to collate the findings from the literature to express the variability in material properties and to attempt to explain the source(s) of the variability. It was found that SFS composition and properties can be highly variable, including different compositions on the exterior and interior of a given SFS particle, which can affect bonding conditions and be one source of variability on composite properties. A suite of tests is proposed to better assess a given SFS stock for potential use in bound applications; at a minimum, the SFS should be evaluated for free CaO content, expansion potential, mineralogical composition, cementitious composite mechanical properties, and chemical composition with secondary tests, including cementitious composite durability properties, microstructural characterization, and free MgO content.

Keywords: steel furnace slag; electric arc furnace slag; basic oxygen furnace slag; ladle metallurgy furnace slag; argon oxygen decarburization slag; concrete

1. Introduction

As a by-product of the various processes of smelting metallic ores, slags are a potentially useful commodity in civil infrastructure applications. Specifically, this review focuses on the use of slags produced from various steelmaking processes. During the production of steel, the initial refinement occurs at a blast furnace, where iron ore is processed to make pig iron. The slag from this process—blast furnace slag—can be used as an aggregate in the form of air-cooled blast furnace slag (ACBFS), but is commonly used as a supplementary cementitious material (SCM) in the form of ground granulated blast furnace slag (GGBFS) [1–5]. However, blast furnace slags will not be covered in this review.

After the blast furnace, the pig iron is refined to produce crude steel. Other crude steels are produced by refining recycled and scrap steel. There are a number of different processes that can be used, and the slag from these processes is broadly termed steel furnace slag (SFS). An estimated 1.8 billion tonnes of crude steel was produced worldwide in 2018 [6], with an estimated worldwide production of 169 to 254 million tonnes of SFS in 2017 [7]. The worldwide effective utilization of SFS is around 80% [8]. The scope of this review is to examine the various types of SFS and how they influence the properties of cementitious composites when used as an aggregate and/or as an SCM. The objective is to reveal that not all SFSs are the same and instead should be classified or qualified according to the intended purpose or use, especially when the SFS is being considered for a bound application, such as concrete, mortar, alkali-activated material, or soil stabilization.

The motivation for this article stems from a previous finding that the type of SFS aggregate can drastically affect the cementitious composite properties when the mixture volumetrics are constant [9,10]. When compared with other recycled aggregates, this finding for SFS has not been clearly explained; for instance, nearly all (if not all) studies of concrete with reclaimed asphalt pavement aggregates have shown a reduction in composite strength and modulus, which has been linked to the development and properties of the concrete microstructure [11,12]. Similarly, concrete with recycled concrete aggregates (RCAs) will typically experience reductions in strength relative to virgin aggregates, but the degree of strength reduction is highly variable, which has been linked to microstructure development, adhered mortar, moisture absorption and content, RCA heterogeneity, quality, and so forth (e.g., [13–17]). In comparison, for SFS aggregates, even for the same SFS type, studies have found that concrete strength can increase, decrease, or be similar to concrete with virgin aggregates. Therefore, this review seeks to collate the existing literature to observe any general trends, to consider sources of variability, and to assess test method(s) to critically analyze SFS for use in cementitious composites.

1.1. Steelmaking Processes

The basic oxygen furnace (BOF), also known as the Linz–Donawitz (LD) process, produces crude steel from the pig iron or molten iron received from the blast furnace. The liquid metal and fluxing agents (e.g., limestone or dolomite) are charged in a furnace, and a lance injects oxygen into the mix, removing impurities from the charge by way of by-product gases, such as carbon monoxide, and by molten slag formation. The molten crude steel is tapped into a ladle, while the molten slag is tapped and removed. In the United States, 30% of the crude steel is produced by the BOF process [18], while around 71% of the worldwide steel production uses the BOF process [6].

The electric arc furnace (EAF) process starts with a cold charge of scrap and recycled steel and fluxing agents. An electric current is passed through graphite electrodes to produce an arc that melts the charge. The injection of oxygen removes impurities, and additional metals or alloyants are added to refine the steel chemistry. The molten crude steel is tapped into a ladle, while the molten slag is tapped and removed. An estimated 29% of steelmaking worldwide uses the EAF process [6], but 70% of the crude steel is produced by the EAF process in the United States [18].

The ladle metallurgy furnace (LMF) is a secondary steelmaking process and is an additional refining step after the BOF or EAF process. The LMF process is similar to the EAF process, except that additional refinements are used. Additional fluxing agents and alloyants are added to the ladle with the molten crude steel to further remove any impurities and to adjust the steel chemistry.

The open-hearth furnace (OHF) process is obsolete and has been largely replaced by the modern BOF and EAF processes. An estimated 0.4% of all steel worldwide is still produced by the OHF process [6].

The argon oxygen decarburization (AOD) process is used for producing stainless and specialty steels. For recycling stainless steels, the process usually starts with an EAF process, which is followed by the AOD process. The AOD process refines the molten metal through decarburization, reduction, and desulfurization. This process results in a slag that is typically very high in calcium and silicon and may contain more fluorine and chromium than EAF and BOF slags [19].

1.2. SFS Composition

Because the various steelmaking processes are different from one another, the resultant SFS chemistry and mineralogy changes. In general, the bulk oxide chemistry of most SFSs consists of CaO, MgO, SiO_2, and FeO, along with some Al_2O_3 and MnO [5,20,21], as shown in Table 1. The mineralogy of the SFS is dependent on the steelmaking process and fluxing agents but is also dependent on the cooling process; the molten SFS can be cooled by air, water spray, water or air quenching, box chilling, and so forth [20]. The cooling process can influence SFS properties and composition, such as degree of crystallinity, particle size, and free CaO and MgO contents [5,20,22–24].

Table 1. Typical SFS composition ranges (in wt.%) [21].

Component	BOF Slag	EAF Slag	Secondary Steelmaking Slag	AOD Slag
CaO	45 to 54	25 to 35	30 to 52	48 to 68
SiO_2	11 to 18	8 to 18	8 to 23	20 to 40
Al_2O_3	1 to 5	3 to 10	3 to 20	1 to 2.5
MgO	1 to 6	2 to 9	6 to 12	4 to 6
Total Fe	14 to 22	20 to 30	0.5 to 12	0.4 to 2
Total Mn	1 to 5	2 to 8	0.5 to 3	0.6 to 1.0 (MnO)
Total Cr	0.1 to 0.3	0.5 to 2.2	<0.1 to 0.5	0.1 to 5 (Cr_2O_3)

The crystalline composition of SFS also varies. One report noted that typical BOF slag compositions by weight consist of 30%–60% dicalcium silicate (with 1%–3% P_2O_5 molar substitution), 0%–30% tricalcium silicate, 0%–10% free CaO (with 2%–10% MnO and 5%–15% FeO molar substitutions), 10%–40% wüstite (with 10%–20% MnO, 10%–30% CaO, and 5%–20% MgO molar substitutions), and 5%–20% dicalcium ferrite [21]. One partial survey of the literature found that the commonly identified minerals in EAF slags are dicalcium silicate, merwinite, gehlenite, iron oxides (wüstite, hematite, and magnetite), mayenite, brownmillerite, and periclase [25]. The same survey found that the commonly identified minerals in BOF slags are dicalcium silicate, tricalcium silicate, wüstite, lime, dicalcium ferrite, portlandite, and calcite [25]. While LMF slag compositions have not been commonly reported, studies have shown dicalcium silicate, tricalcium silicate, wüstite, mayenite, periclase, bredigite, and merwinite to be present [9,10,26,27].

One of the factors limiting the use of SFS is the expansion potential. SFS often contains free CaO and free MgO, which expand by 92% and 120%, respectively, when reacted with water [28]. The typical free CaO content ranges for BOF and EAF slags are 1%–10% and 0%–4%, respectively [21]. The free CaO and free MgO are present primarily due to the fluxing agents and the furnace refractory lining [20].

2. Concrete and Mortar with SFS Aggregates

As the SFS quality and composition can vary based on the steelmaking process, it can perhaps be expected that the properties of mortars and concrete containing SFS aggregates would be variable as well. Table 2 is a summary of the literature, highlighting the effect on a given property for specific SFS aggregates used as a partial to full replacement of the virgin fine and/or coarse aggregates in mortar and concrete. The majority of studies have concerned the use of EAF or BOF slag aggregates, with few studies considering LMF or AOD slag aggregates and no studies using OHF slag aggregates. The majority of studies have focused on mechanical properties, such as strength and elastic modulus, and few studies have considered the effect of SFS aggregates on durability properties.

It is clear from Table 2 that there are variable trends for a given SFS type. For instance, 51 studies were identified to have considered the compressive strength of cementitious composites when using EAF slag aggregates, of which 37 studies (72%) showed an increase in strength, 4 studies (8%) showed a decrease in strength, and 10 studies (20%) showed no change in strength when compared with a control. Similarly, for compressive strength with BOF slag aggregates, of 27 studies, the distribution was 52%, 30%, and 18% for increase, decrease, and no change, respectively. Therefore, for a given stockpile of EAF or BOF slag aggregates, what is the probability that the SFS aggregate will increase the compressive strength relative to a control? For quality assurance concerns, this is an important consideration since it is impractical to perform all mechanical and durability tests on all stockpiles of all SFS aggregates. However, it should be noted that Table 2 does not attempt to factor in other effects on concrete properties, such as water-to-cementitious ratio, cement content, age, curing conditions, use of SCMs, SFS replacement amount, coarse vs. fine aggregate replacements, gradation effects, control mixture, virgin aggregate type, and so forth. Therefore, the conclusions drawn from Table 2 should remain fairly general.

Table 3 details the use of SFS aggregates in geopolymer and alkali-activated concretes. Significantly fewer studies have been performed on SFS aggregates in geopolymer and alkali-activated concretes (Table 3) than portland cement composites (Table 2), although the trends more clearly suggest a positive effect on strength; for compressive strength, of 25 studies identified, 20 studies (80%) indicated that SFS aggregates can increase strength.

3. SFS as a Cementitious Material

Even though SFS often contains dicalcium silicate and sometimes tricalcium silicate, these phases are not always reactive. The dicalcium silicate in SFS can be present as the β and/or γ polymorphs [20,29]. While β-dicalcium silicate is present and reactive in portland cements [30], it is reportedly relatively nonreactive in SFS [31], and γ-dicalcium silicate is not a hydraulic mineral phase [32]. However, some studies have shown evidence of hydration of the calcium silicate phases in SFS [33,34], while other studies have shown evidence of hydration of the calcium aluminate phases [35,36]. In addition, both free CaO and free MgO present in the SFS are hydraulic, which could contribute to the hydration of portland cement when SFS is used as an SCM. In general, the use of SFS as an SCM will be detrimental to the mechanical properties of cementitious composites [37], which is somewhat evident in Table 4. While Table 4 demonstrates that some SFS studies indicate a usefulness as an SCM, it is clear that not all studies conclude with this finding. Since SFS can have variable chemistry and mineralogy, it is perhaps not surprising that the hydraulic or pozzolanic reactivity is also variable. Therefore, to assess the relative reactivity of a given SFS, the mineralogy of the slag should be assessed (see Section 5.1) to determine whether any reactive phases are present. A pozzolanic reactivity test can also be performed [38].

High pH solutions will accelerate the hydration of SFS [39], so instead of using it as an SCM in portland cement composites, SFS has also been considered for alkali-activated binders. Favorable performance has been reported for alkali-activated binders using LMF slags [40–43], EAF slags [43], BOF slags [44], and stainless steel slags [45–48]. BOF and LMF slags have also been suggested as activators for GGBFS pastes [49,50].

SFS has also been considered for use in soil stabilization, as shown in Table 4. Specifically, due to the potentially high free CaO and free MgO contents in SFS and since lime is known to chemically react with clays [51–55], SFS has the potential to act as a clayey soil stabilizer. In addition, the discussion of SFS as an SCM revealed that calcium silicate and/or calcium aluminate phases present in the SFS may contribute to the reaction. In general, Table 4 indicates the favorable effects of using SFS in soil stabilization, which can be attributable, at least in part, to chemical reactions. In addition, some studies have suggested that a mechanical stabilization mechanism may contribute as well owing to the angularity and roughness of the SFS particles. It is unclear which stabilization mechanism(s) is dominating, as it is likely a function of multiple factors, such as SFS chemistry, mineralogy, reactivity, shape and texture, particle size distribution, and so forth.

Table 2. Effect of SFS used as a partial to full replacement of virgin coarse and/or fine aggregate in portland cement concrete relative to the control with virgin aggregates.

Property	EAF Slag		
	Increase	**Decrease**	**No Change**
Compressive strength	[9,10,34,56–90]	[82,91–93]	[94–102]
Split tensile strength	[10,58–61,65,69,70,73,74,77,78,82,84–86,90,101]	[9,75,76]	[87,93,96,97,102]
Flexural strength	[60–63,69,70,73,74,77,83–85,88]	[92,100]	[75,97,98,101,103]
Modulus of elasticity	[59,60,62,64,66,73,74,77,82,85,86,90,97,101]	[75,82,83]	[67,75,87,94,96,98]
Dynamic modulus	[10,63,65,77,103]		[67]
Stress intensity factor	[9,84]		
Total fracture energy	[9,60,83,84]	[65]	
Free drying shrinkage	[9,65,74,89]	[100,101,104,105]	[67,70,102]
Water absorption	[56,57,73,76,87,98]	[78,99,101]	[70,79,102]
Freeze/thaw durability	[56,62,63,70,86,90,99,104]		[60,98,102]
Wetting/drying durability	[56,60,62,73,74,77,90,100,104]	[86,106]	[102,107]
Abrasion resistance	[60,69–71,73,78]		
High-temperature resistance	[83,108]	[70,75,76]	
Porosity	[56,60,63,68,77,87,94,102]		
Workability and fresh properties	[58,62,65,69,76,86,87,97]	[9,61,85,86,109]	
Density and specific weight	[9,56–58,60,62,65,66,70,76,85–87,90,97,102]		
Shear capacity	[85,88]		
Expansion	[63,73,79]	[57,86,110,111]	

Property	BOF and LD Slag			LMF Slag		
	Increase	**Decrease**	**No Change**	**Increase**	**Decrease**	**No Change**
Compressive strength	[33,34,80,112–122]	[9,10,81,123–126]	[95,105,127–129]	[10,80,81,130–132]	[26,27,133]	[102,134,135]
Split tensile strength	[115,116]	[9,10]		[10,134]		[102]
Flexural strength	[115,116,136]		[128]	[132]		
Modulus of elasticity	[115]		[105]			
Dynamic modulus	[10]			[10]		
Stress intensity factor	[9]					
Total fracture energy	[9]					
Free drying shrinkage	[9]	[124]			[131]	[102]
Water absorption	[124,137]	[105,115]	[116]		[115]	[102]
Freeze/thaw durability		[137]	[29,112,114,116,137]	[130,132]		[102]
Wetting/drying durability			[105,112]		[131]	[102]
Abrasion resistance	[137]	[112]	[105]			
High-temperature resistance						
Porosity	[105,118]	[116]	[126]	[102]		
Workability and fresh properties	[138,139]	[9]	[114]			
Density and specific weight	[9,80,105,115,116,122,126]					
Shear capacity						
Expansion	[125,126,140]	[112,117,126]	[116]			

Table 2. *Cont.*

Property	AOD Slag and Other Stainless Steel Slags			Other Steel Slags or Unspecified		
	Increase	**Decrease**	**No Change**	**Increase**	**Decrease**	**No Change**
Compressive strength	[63,141–143]	[26,144,145]	[146]	[78,87,147–162]	[111,163–169]	[170–175]
Split tensile strength	[63]			[78,149–151,153,156,157,160]	[148,163–165]	[171,174]
Flexural strength		[144]		[147–151,154,158,159]	[111,163–165]	[170,171,173,175]
Modulus of elasticity				[147,150,151,156,159,162]	[111]	[171,173]
Dynamic modulus	[63]			[157,162]	[165]	
Stress intensity factor				[150]		
Total fracture energy						
Free drying shrinkage					[111]	[168]
Water absorption	[142]	[144]		[153,164,167,168]	[147,171]	[78,155,157–160]
Freeze/thaw durability	[142]				[164]	
Wetting/drying durability					[148]	
Abrasion resistance	[144]			[78,147,150,154,157,159–161,170,171]	[165]	
High-temperature resistance				[173]		
Porosity				[167]		
Workability and fresh properties				[175]		
Density and specific weight				[158–160,165]	[147]	
Shear capacity						
Expansion	[141]	[142]				[175]

Table 3. Effect of SFS used as a partial to full replacement of virgin coarse and/or fine aggregate in geopolymer or alkali-activated mortars or concretes relative to the control with virgin aggregates.

Property	EAF Slag			BOF and LD Slag			LMF Slag		
	Increase	**Decrease**	**No Change**	**Increase**	**Decrease**	**No Change**	**Increase**	**Decrease**	**No Change**
Compressive strength	[176–178]		[179]	[180]	[126]		[40,41,181–183]		
Split tensile strength	[179]								
Flexural strength	[179]			[180]					
Modulus of elasticity	[176]								
Shrinkage		[176,178]			[180]				
Abrasion resistance	[177]								
Water Absorption									
Freeze/thaw resistance					[180]				

Property	AOD Slag and Other Stainless Steel Slags			Other Steel Slags or Unspecified		
	Increase	**Decrease**	**No Change**	**Increase**	**Decrease**	**No Change**
Compressive strength	[45–47]			[184–191]	[192,193]	[194]
Split tensile strength				[186,188]	[192]	
Flexural strength				[186,187,189,190]	[192]	
Modulus of elasticity				[186]	[192]	
Shrinkage					[190]	
Abrasion resistance				[193]		
Water absorption				[190,193]	[186]	
Freeze/thaw resistance					[192]	

Table 4. Effect of SFS as a supplementary cementitious material or a soil stabilizer.

SFS Type	Effect	Effectiveness as a Supplementary Cementitious Material	Effectiveness as a Soil Stabilizer
EAF Slag	Increase	[95,152,195]	[196–201]
	Decrease	[95,133]	
	No change	[202]	
BOF and LD Slag	Increase	[33,115,203–207]	[208–213]
	Decrease	[38,214,215]	
	No change	[128,216,217]	
LMF Slag	Increase	[134]	[218–222]
	Decrease	[26,27,38,223–225]	
	No change		
AOD and Stainless Steel Slag	Increase	[226]	
	Decrease	[26]	
	No change		
Other Steel Slags or Unspecified	Increase	[227–230]	[155,231–241]
	Decrease	[167,242–246]	
	No change	[243,247,248]	[249,250]

4. Discussion of SFS Variability

Certainly, Tables 2–4 present a view of SFS that there can be significant variability in composite materials' behavior. First and foremost, this variability stems from different steelmaking processes (e.g., EAF, BOF, LMF, AOD), different steel chemistries, different slag cooling methods, different fluxing agents, and so forth. Therefore, each stockpile of SFS can have variable chemical composition, mineralogical composition, free CaO content, free MgO content, particle size distribution, particle shape and texture, porosity, and so forth.

Table 5 shows an example dataset from the literature where the same concrete mix design was used with equivalent volumetric replacements of the coarse aggregate by EAF slag or BOF slag relative to a control. In this example, the compressive strength increased with EAF slag but decreased with BOF slag, while both SFS aggregates increased the fracture properties and free drying shrinkage [9]. In a subsequent study, these same aggregates were investigated by backscattered electron microscopy, and it was found that the BOF slag aggregates exhibited a larger, more porous interfacial transition zone (ITZ) than the EAF slag or dolomite aggregates, which exhibited similar ITZ characteristics [10]. By microscopic analysis, the BOF slag was also found to exhibit a different surface composition than the interior, while the EAF slag did not exhibit a different surface composition, which was seen to be one explanation why the BOF slag reduced compressive strength while EAF slag increased strength in Table 5. Table 6 shows a related dataset for mortars with equivalent volumes of dolomite, EAF slag, BOF slag, or LMF slag aggregates, where it can be seen again that EAF slag achieved greater mechanical properties than the control, whereas BOF and LMF slag aggregates experienced reductions in strength, possibly attributable to the surface composition. The different exterior and interior compositions of SFS particles have been shown for BOF and LMF slags [10,114,123,251] but not EAF slag [10,251]. For BOF slag, Kawamura et al. reported an exterior particle surface composition containing calcite, calcium silicate hydrate, and calcium carboaluminate hydrate phases, which was argued to result in a reduced paste aggregate bond [123]. Similar arguments can be made for aged vs. unaged SFS aggregates, since the properties of SFS aggregates will change when they are aged, weathered, or carbonated, such as reduction in aggregate porosity [114,169], decrease in pH [121,124,252,253], decrease in chemically absorbed water [124], and alteration of the aggregate surface texture and composition [121,169,254–257]. Conversely, increases in concrete strength when using SFS aggregates have been argued to be attributable to the rough particle surface texture and

possibly chemical reactions occurring in the cement paste and the SFS particle, such as for BOF slag [113], EAF slag [9], or other or unspecified SFS [151,154] aggregates.

Table 5. Twenty-eight-day concrete properties (average ± standard deviation) for three equivalent mixes with full replacement of coarse aggregate with dolomite (control), EAF slag, or BOF slag [9].

Mix	Compressive Strength (MPa)	Critical Mode I Stress Intensity Factor (MPa-m$^{1/2}$)	Total Fracture Energy (N/m)	Free Drying Shrinkage (με)
Control	46.1 ± 1.4	1.00 ± 0.12	101.6 ± 15.9	−437 ± 21
EAF	48.3 ± 0.5	1.39 ± 0.06	124.0 ± 8.1	−517 ± 55
BOF	40.1 ± 2.0	1.21 ± 0.06	118.5 ± 6.5	−537 ± 60

Table 6. Twenty-eight-day mortar properties (average ± standard deviation) for four equivalent mixes with full replacement of aggregate with matched gradations of dolomite (control), EAF slag, BOF slag, or LMF slag [10].

Mix	Compressive Strength (MPa)	Split Tensile Strength (MPa)	Longitudinal Dynamic Modulus (GPa)
Control	41.1 ± 2.2	4.5 ± 0.4	32.9 ± 1.0
EAF	49.8 ± 2.2	5.1 ± 0.6	43.6 ± 0.5
BOF	38.5 ± 1.1	4.3 ± 0.7	40.4 ± 1.8
LMF	43.0 ± 4.3	5.1 ± 0.3	41.3 ± 1.1

Lastly, the variability in concrete behavior with SFS aggregates could be attributable to the aggregate absorption capacity and absorption. Particularly for aggregates with high absorption capacities, improperly accounting for the moisture content can drastically affect concrete properties and microstructure development (e.g., [13,14]). The absorption capacity of SFS aggregates is typically ≤4% [258–260], with coarse and fine SFS aggregates typically ranging 1–2% and 2–4%, respectively [260]. As these values are comparable to conventional virgin aggregates, variability in concrete properties may not be significant, provided that the moisture content is accommodated during the mix design and batching processes.

5. Requirements for SFS Characterization

Given that a given type of SFS aggregate can have variable effects on concrete properties (Table 2), it is evident that the aggregate should be characterized to assess its suitability for use in bound applications. This section presents a number of characterization techniques and their relative usefulness in qualifying a given SFS source for a given application. A number of characterization techniques are recommended, particularly if the potential for deleterious expansion is of concern.

5.1. Chemical and Mineralogical Characterization

The chemical composition alone should not be used as a predictor of SFS behavior, since there is often substantial elemental substitution. A combination of chemical and mineralogical classifications will initiate a more complete analysis of the SFS chemical properties.

The chemical composition of SFS is typically assessed by X-ray fluorescence (XRF), inductively coupled plasma optical emission spectrometry (ICP-OES), atomic absorption spectroscopy (AAS), or a combination thereof [19,261–266]. Typically, these data are represented in the oxide form, as shown in Table 1.

The crystalline mineral composition of SFS can be assessed by X-ray diffraction (XRD) [263,264,266–268]. Very commonly, XRD is used to qualitatively assess the SFS composition, as discussed in Section 1.2 with typical mineral compositions. While there is a list of minerals commonly identified in SFS (e.g., larnite, wüstite, hematite, brownmillerite, lime, merwinite, and periclase), the composition can vary with a wide range of minor or trace compounds; for instance, one partial

review of the literature found 59 different mineral compounds reported for various EAF and BOF slags [25], which demonstrates the need for mineralogical characterization for SFS.

One complication with laboratory XRD is that Cu Kα radiation is very common, which will induce fluorescence in iron and iron-containing minerals [269], resulting in a higher background in the diffractogram. The higher background may overwhelm smaller peaks (i.e., present for low phase contents, poorly crystalline phases, etc.), diminishing the accuracy of qualitative or quantitative XRD analysis. The typical phase detection limit for powder XRD is reported to be around a few percent up to 10% [270–272]. Therefore, for XRD experiments where fluorescence is a potential issue, it is important to consider an appropriate X-ray source [273]. For SFS and iron-containing minerals, Co Kα or Cr Kα, for instance, has shown to be more reliable [33,267–269,274]; indeed, quantitative XRD, such as by Rietveld analysis, is possible for SFS by using Co Kα radiation [33,268]. Quantitative XRD can also be used to estimate the relative amounts of each crystalline phase and amorphous phase(s) [275].

5.2. Free CaO Content

If the free CaO content is not high enough to be reasonably estimated by quantitative XRD, then another useful test is complexometric titration. Originally developed to determine the free CaO content in portland cement and clinker [276–278], this method uses hot ethylene glycol to complex with the free CaO, making it applicable to SFS [9,29,113,279–284]. However, the hot ethylene glycol complexes with Ca^{2+} from both free CaO and $Ca(OH)_2$, so Brand and Roesler [9] proposed using thermogravimetric analysis (TGA) to determine the $Ca(OH)_2$ content to refine the estimate of the actual free CaO content.

The available Ca^{2+} ions from the free CaO and $Ca(OH)_2$ form a complex with the ethylene glycol, thereby shifting the pH of the solution. Using phenolphthalein as an indicator, an acid is titrated into the solution until the pH is adjusted. Previous SFS studies have shown that ethylene glycol at 95 ± 5 °C mixed with a powdered SFS sample for 30 min is sufficient [9,279]. The equation to determine the free CaO content is [277]:

$$EGN = F\left[\frac{N(V - V_b)}{10\ m}\right], \quad (1)$$

where EGN is the ethylene glycol number that needs to be corrected based on the estimated $Ca(OH)_2$ content, F is a correction factor, m is the initial mass of the SFS sample (g), N is the normality of the acidic solution, V is the volume of acidic solution titrated (mL), and V_b is a correction for the volume of acidic solution titrated in a blank ethylene glycol sample (mL). For this configuration, the correction factor F is 28 [9,277,279,285]. Typically, V_b is 0 mL. Previous studies have shown that 0.05 N to 0.1 N hydrochloric acid is a reasonable solution for titration [9,279,283] since the volume titrated provides suitable resolution in the measurement (e.g., a very strong acid would not require much volume to titrate, which means that the volume titrated may be easily overestimated).

However, one complication of the ethylene glycol method is that the free CaO is not fully complexed by ethylene glycol if it has formed as a solid solution with 20% or more by mass with other divalent metal oxides (e.g., MgO, FeO, MnO) [286].

5.3. Free MgO Content

There is no commonly applied MgO equivalent to the ethylene glycol test for CaO, so free MgO can be difficult to estimate. Some selective extraction methods have been proposed, such as with potassium dichromate [287], ammonium nitrate [288], or ethylene glycol with iodine and ethanol [289,290], while other studies proposed solid-state ^{25}Mg nuclear magnetic resonance spectroscopy [291] or petrographic methods [292], but their data are limited. However, the free MgO content is very important to estimate, because the MgO reaction with water is a longer-term reaction than CaO, resulting in the potential for unexpected failures at later ages. If the free MgO content is high enough, then quantitative XRD could provide a reasonable estimate [267,268]. Alternatively, a method proposed by Brand and Roesler [9] uses TGA to estimate the $Mg(OH)_2$ content in an SFS sample that was exposed

to autoclave conditions to convert all free MgO to $Mg(OH)_2$. Microwave irradiation has also been proposed to rapidly convert all free MgO to $Mg(OH)_2$ [293]. From the $Mg(OH)_2$ content, the initial free MgO content can be estimated by stoichiometric conversion. For the BOF 1, EAF 1, and LMF 1 samples in Table 7, the free MgO contents were estimated by this method to be 2.2%, 0.2%, and 0.3%, respectively [9].

Table 7. Estimated total free CaO contents based on titration and TGA [9,222,279].

SFS Type	EGN Value from Titration (%)	$Ca(OH)_2$ Content from TGA (%)	Stoichiometric CaO Content in $Ca(OH)_2$ (%)	Estimated Free CaO Content (%)
BOF 1	4.4	1.3	1.0	3.4
EAF 1	0.1	0.0	0.0	0.1
LMF 1	0.5	0.2	0.1	0.4
LMF 2	3.5	1.3	1.0	2.5
SFS 1 *	4.0	1.4	1.1	2.9
SFS 2 *	3.7	1.1	0.8	2.9
SFS 3 *	5.1	1.1	0.9	4.2

* Unknown SFS type but suspected to be BOF.

One complication with assessing free MgO content is that the SFS can contain a solid solution of MgO and FeO (i.e., magnesiowüstite), making the exact quantification of free MgO difficult [294].

5.4. Expansion Potential

Given the volumetric expansion when free CaO and free MgO hydrate, SFS aggregates can exhibit significant expansion, as has been demonstrated in a number of failure case studies (e.g., [295–300]). While the primary expansion issues are attributed to the hydration of free CaO and free MgO, additional expansion effects have been argued to be attributable to the conversion of β-dicalcium silicate to γ-dicalcium silicate, oxidation of FeO to Fe_3O_4, carbonation of oxide or hydroxide phases, hydration of silicate or sulfide phases, and/or rust formation from metallic inclusions [294]. Additional hydration products have also been identified, such as calcium monocarboaluminate, calcite, hexagonal calcium aluminate hydrates, hydrogarnet, and calcium silicate hydrate [39,114,123,251], although it is unclear if and how much these additional hydration products contribute to expansion.

Based on the expansion potential, it is recommended that granular SFS undergo some form of an expansion test, a number of which have been proposed in the literature, some examples of which include the following:

- *Autoclave expansion test (unbound SFS).* This rapid expansion test of unbound SFS aggregates uses the ASTM C151 autoclave procedure (steam at 300 psi (2.1 MPa) and 420 °F (215 °C) for 3 h) [9,258,279,301]. The SFS sample is compacted in a steel mold and exposed to the autoclave conditions with an applied surcharge. The height of the surcharge before and after autoclaving is measured to calculate a percent expansion. While this expansion value does not necessarily correlate well to field performance or free CaO content, it is a very rapid test method that can be used as an index test. In addition, autoclaving conditions can be used to study the hydration reactions in SFS [302,303].
- *Autoclave expansion test (bound SFS).* Inspired by the ASTM C151 autoclave test also, some researchers have used an autoclave to study the expansion of cementitious pastes, mortars, or concretes with SFS [56,89,126,242,304]. The concept of this test is to accelerate the expansive reaction(s) in the SFS, so it is also useful as an index test or as a test to simulate rapid weathering.
- *Expansion force test.* Wang [136] developed this test for unbound SFS coarse aggregates as a method to compute the expansion force generated by a single SFS aggregate bound in a rigid matrix such as concrete. In this test, compacted unbound SFS aggregates are compacted in a cylindrical mold and submerged in water at 74 °C (165 °F), and a load cell is used to monitor the force exerted by

the expanding aggregate. From these data, the tensile stresses induced by a single expanding SFS particle can be computed, which can be used to assess the "usability criteria" of the SFS aggregates to be used in bound applications [5].

- *Disruption ratio test*. This test also uses autoclave conditions but determines the percentage of SFS aggregates that cracked or powdered after autoclaving [136]. This test can be used as a rapid indexing test for volumetric stability of SFS aggregates.
- *ASTM D4792 "Standard Test Method for Potential Expansion of Aggregates from Hydration Reactions."* In this test method, unbound aggregates are compacted in a cylindrical mold and then submerged in 70 °C (158 °F) water, and the expansion is measured over time. This test has been shown to be effective as a comparative or an index test to assess relative expansion of SFS [305–308]. For use as a graded material in pavement bases, ASTM D2940 recommends that the expansion of SFS aggregates should be ≤0.50% by ASTM D4792.

Because of the potential for significant expansion, some researchers have proposed pretreating the SFS prior to its use as an aggregate in bound applications, such as by outdoor weathering [56,79,99,309–311], carbonation [114,121,124,152], steam aging [79,129,311,312], and so forth. The expansion tests detailed above are suitable candidates to confirm the degree of reaction or expansion before using the SFS.

5.5. Microstructural Assessment

Microstructural analysis of polished SFS sections can be effective to better assess the phase distribution, such as with scanning electron microscopy (SEM) with backscattered electron (BSE) imaging and mapping with energy dispersive X-ray (EDX) spectroscopy [10,24,66,251,264,281,313–315]. This technique has also proven to be effective in evaluating that the surface of SFS particles may be different from the particle interior [10,251], as exampled in Figure 1, which could be a contributing factor in how concrete with SFS aggregates behaves, as discussed in Section 4. Optical microscopy of polished sections has also been demonstrated to be effective at characterizing the phases present in SFS samples [264,292,313]. Coupling SEM/EDX with XRD data allows for a more detailed compositional and corroborative analysis.

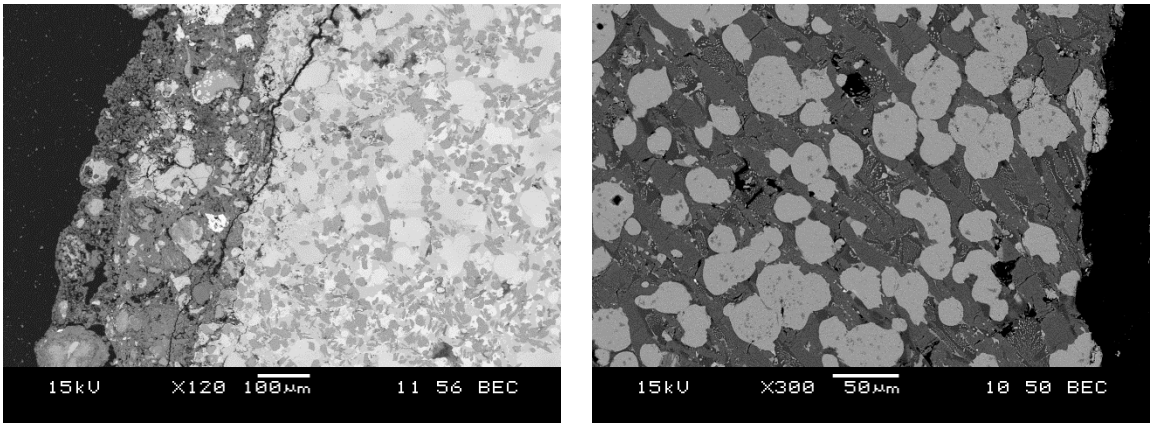

(**a**) (**b**)

Figure 1. Compositional BSE micrographs at the edge of a (**a**) BOF slag and (**b**) EAF slag particle. The BOF slag particle exhibited a surface composition that was compositionally different from the interior of the particle, whereas the EAF slag particle appeared to have similar surface and interior compositions.

6. Recommendations

Because of different production processes, fluxing agents, steel chemistries, and so forth, the properties of SFS can vary greatly. Therefore, to qualify a given SFS stock for use as aggregate in

concrete or other bound applications, it is recommended that the following tests be performed at a minimum, listed in order of suggested importance:

1. *Free CaO*. The hydration of CaO yields a volume expansion of 92% and reacts quicker than free MgO. Initial or early-age expansion can be expected to be attributable to free CaO. Therefore, estimating the free CaO content is a rapid method to quickly assess an expansion potential. The common method to evaluate free CaO content is with ethylene glycol extraction and complexometric titration, which can also be coupled with TGA to provide a more precise quantification of free CaO and $Ca(OH)_2$.
2. *Expansion test*. The most concerning effect of using SFS in bound applications is expansion that can result in structural failure. A number of accelerated and long-term expansion tests have been proposed in the literature, so the data are insufficient to recommend a specific test method. The allowable expansion depends on the specific application of SFS, so no limits are recommended. For the routine utilization of SFS, one recommendation is to select a specific expansion test and develop a testing history to empirically determine what limit(s) is permissible for a given application. Accelerated expansion tests can also be used to rapidly screen a given SFS stock, such as to track weathering progress.
3. *Mineral composition*. Qualitative XRD can be used to quickly identify the presence of crystalline phases that can be involved in deleterious reactions. Quantitative XRD can be used to determine the relative amounts of crystalline and amorphous phases. Due to fluorescence issues with Cu Kα radiation and iron-bearing phases, an appropriate anode should be considered, such as Co Kα radiation.
4. *Concrete mechanical properties*. In conjunction with the above recommended tests, the mechanical properties of concrete with SFS aggregates should be tested to confirm whether or not the design minimum properties are met. Given that the SFS aggregates can have a varied effect on concrete mechanical properties, as demonstrated in Table 2, testing the concrete mechanical properties can quickly screen a given SFS stock for appropriateness as an aggregate.
5. *Chemical composition*. The elemental composition of the SFS should be assessed, particularly if heavy metals are of concern. However, this composition is arguably not as useful as the other tests since it does not provide any information on expansion potential (e.g., there is no distinction between Ca in free CaO and bound in a mineral phase).

In addition to the above tests, further recommended testing can be conducted if needed. These secondary tests include the following, listed in order of suggested importance:

1. *Concrete durability properties*. Given that the SFS aggregates can have a varied effect on concrete durability properties, as demonstrated in Table 2, various tests can be performed to assess and predict the performance of the concrete. The specific tests should be selected based on the expected environmental conditions of the in-service concrete. If SFS expansion may be an issue, based on the results of the recommended primary tests above, then both early-age and long-term durability properties should be assessed to consider hydration of free CaO and free MgO, respectively.
2. *Microstructural characterization*. The facilities and equipment are more costly and perhaps not as readily available as some of the other recommended tests, which is why it is not included in the primary testing list. However, microstructural characterization, with either electron or optical microscopy methods, has demonstrated that SFS is heterogeneous and that the outer SFS particle composition can be different from the inner particle composition. Therefore, microstructural characterization of SFS particles or of concrete with SFS aggregates can assist in determining bonding conditions and failure mechanisms.
3. *Free MgO*. The hydration of MgO yields a volume expansion of 120% and reacts slower than free CaO. Long-term or late-age expansion can be expected to be attributable to free MgO. While this would be an important metric for assessment, there are insufficient data in the literature on which

test(s) is most accurate or efficient. Further study and validation is needed to produce a testing methodology with equivalent widespread use and reliability as the tests for free CaO.

7. Conclusions

Steel furnace slag (SFS) is generated from a number of different processes and can generally be categorized as electric arc furnace (EAF) slag, basic oxygen furnace (BOF) slag, ladle metallurgy furnace (LMF) slag, or argon oxygen decarburization (AOD) slag. When used as an aggregate or in powdered form for various cementitious applications, such as concretes, mortars, alkali-activated materials, or soil stabilization, the literature demonstrates that the effects on material properties can be highly variable, which means that predicting effects on material properties is very difficult. The source of the variable effects can be somewhat attributable to the variability in SFS composition; for instance, the exterior and interior of a given SFS particle can have different compositions, which may affect bonding conditions and thereby influence composite performance.

To better qualify a given SFS stock for use in cementitious applications, a suite of tests is proposed. Specifically, a primary set of tests is recommended, including free CaO content, expansion potential, mineralogical composition, cementitious composite mechanical properties, and chemical composition, with a secondary set of tests, including cementitious composite durability properties, microstructural characterization, and free MgO content. The primary set of tests is recommended as testing that should definitely be performed during SFS assessment, while the secondary set of tests, while also useful, may not always be applicable or be easily performed.

Author Contributions: Conceptualization, A.S.B.; formal analysis, A.S.B. and E.O.F.; writing—original draft preparation, A.S.B. and E.O.F.; writing—review and editing, A.S.B. and E.O.F.; supervision, A.S.B. All authors have read and agreed to the published version of the manuscript.

Funding: This research received no external funding.

Conflicts of Interest: The authors declare no conflict of interest.

References

1. Özbay, E.; Erdemir, M.; Durmuş, H.İ. Utilization and efficiency of ground granulated blast furnace slag on concrete properties—A review. *Constr. Build. Mater.* **2016**, *105*, 423–434. [CrossRef]
2. Shi, C.; Qian, J. High performance cementing materials from industrial slags—A review. *Resour. Conserv. Recycl.* **2000**, *29*, 195–207. [CrossRef]
3. Snellings, R.; Mertens, G.; Elsen, J. Supplementary cementitious materials. *Rev. Mineral. Geochem.* **2012**, *74*, 211–278. [CrossRef]
4. Buddhdev, B.G.; Timani, K.L. Critical review for utilization of blast furnace slag in geotechnical application. In *Problematic Soils and Geoenvironmental Concerns*; Latha Gali, M., Raghuveer Rao, P., Eds.; Springer: Singapore, 2021; pp. 87–98. [CrossRef]
5. Wang, G.C. *The Utilization of Slag in Civil Infrastructure Construction*; Woodhead Publishing: Cambridge, UK, 2016. [CrossRef]
6. World Steel Association. *World Steel in Figures*; World Steel Association: Brussels, Belgium, 2019.
7. van Oss, H.G. Slag–Iron and steel. In *2017 Minerals Yearbook*; U.S. Geological Survey: Reston, VI, USA, 2017; pp. 69.1–69.8.
8. Branca, T.A.; Colla, V.; Algermissen, D.; Granbom, H.; Martini, U.; Morillon, A.; Pietruck, R.; Rosendahl, S. Reuse and recycling of by-products in the steel sector: Recent achievements paving the way to circular economy and industrial symbiosis in Europe. *Metals* **2020**, *10*, 345. [CrossRef]
9. Brand, A.S.; Roesler, J.R. Steel furnace slag aggregate expansion and hardened concrete properties. *Cem. Concr. Compos.* **2015**, *60*, 1–9. [CrossRef]
10. Brand, A.S.; Roesler, J.R. Interfacial transition zone of cement composites with steel furnace slag aggregates. *Cem. Concr. Compos.* **2018**, *86*, 117–129. [CrossRef]
11. Brand, A.S.; Roesler, J.R. Bonding in cementitious materials with asphalt-coated particles: Part I—The interfacial transition zone. *Constr. Build. Mater.* **2017**, *130*, 171–181. [CrossRef]

12. Brand, A.S.; Roesler, J.R. Bonding in cementitious materials with asphalt-coated particles: Part II—Cement-asphalt chemical interactions. *Constr. Build. Mater.* **2017**, *130*, 182–192. [CrossRef]
13. Brand, A.S.; Roesler, J.R.; Salas, A. Initial moisture and mixing effects on higher quality recycled coarse aggregate concrete. *Constr. Build. Mater.* **2015**, *79*, 83–89. [CrossRef]
14. Brand, A.S.; Roesler, J. Interfacial transition zone of cement composites with recycled concrete aggregate of different moisture states. *Adv. Civ. Eng. Mater.* **2018**, *7*, 87–102. [CrossRef]
15. Jayasuriya, A.; Adams, M.P.; Bandelt, M.J. Understanding variability in recycled aggregate concrete mechanical properties through numerical simulation and statistical evaluation. *Constr. Build. Mater.* **2018**, *178*, 301–312. [CrossRef]
16. Etxeberria, M.; Vázquez, E.; Marí, A.; Barra, M. Influence of amount of recycled coarse aggregates and production process on properties of recycled aggregate concrete. *Cem. Concr. Res.* **2007**, *37*, 735–742. [CrossRef]
17. González-Taboada, I.; González-Fonteboa, B.; Martínez-Abella, F.; Carro-López, D. Study of recycled concrete aggregate quality and its relationship with recycled concrete compressive strength using database analysis. *Mater. Construcción* **2016**, *66*, e089. [CrossRef]
18. U.S. Geological Survey. *Mineral Commodity Summaries 2020*; U.S. Geological Survey: Reston, VI, USA, 2020.
19. Jung, S.-M.; Sohn, I.; Min, D.-J. Chemical analysis of argon–oxygen decarburization slags in stainless steelmaking process by X-ray fluorescence spectrometry. *X-Ray Spectrom.* **2010**, *39*, 311–317. [CrossRef]
20. Shi, C. Steel slag—Its production, processing, characteristics, and cementitious properties. *J. Mater. Civ. Eng.* **2004**, *16*, 230–236. [CrossRef]
21. Balcázar, N.; Kühn, M.; Baena, J.M.; Formoso, A.; Piret, J. *Summary Report on RTD in Iron and Steel Slags: Development and Perspectives*; Proceedings No. EUR 19066 EN; European Commission: Luxembourg, 1999.
22. Tossavainen, M.; Engstrom, F.; Yang, Q.; Menad, N.; Lindstrom Larsson, M.; Bjorkman, B. Characteristics of steel slag under different cooling conditions. *Waste Manag.* **2007**, *27*, 1335–1344. [CrossRef]
23. Loncnar, M.; Mladenovič, A.; Zupančič, M.; Bukovec, P. Comparison of the mineralogy and microstructure of EAF stainless steel slags with reference to the cooling treatment. *J. Min. Metall. Sect. B Metall.* **2017**, *53*, 19–29. [CrossRef]
24. Engström, F.; Adolfsson, D.; Yang, Q.; Samuelsson, C.; Björkman, B. Crystallization behaviour of some steelmaking slags. *Steel Res. Int.* **2010**, *81*, 362–371. [CrossRef]
25. Brand, A.S.; Roesler, J.R. *Concrete with Steel Furnace Slag and Fractionated Reclaimed Asphalt Pavement*; Report No. ICT-14-015; Illinois Center for Transportation: Urbana, IL, USA, 2014.
26. Kriskova, L.; Pontikes, Y.; Cizer, Ö.; Mertens, G.; Veulemans, W.; Geysen, D.; Jones, P.T.; Vandewalle, L.; Van Balen, K.; Blanpain, B. Effect of mechanical activation on the hydraulic properties of stainless steel slags. *Cem. Concr. Res.* **2012**, *42*, 778–788. [CrossRef]
27. Shi, C. Characteristics and cementitious properties of ladle slag fines from steel production. *Cem. Concr. Res.* **2002**, *32*, 459–462. [CrossRef]
28. Erlin, B.; Jana, D. Forces of hydration that can cause havoc in concrete. *Concr. Int.* **2003**, *25*, 51–57.
29. Gupta, J.D.; Kneller, W.A.; Tamirisa, R.; Skrzypczak-Jankun, E. Characterization of base and subbase iron and steel slag aggregates causing deposition of calcareous tufa in drains. *Transp. Res. Rec.* **1994**, *1434*, 8–16.
30. Taylor, H.F.W. *Cement Chemistry*, 2nd ed.; Thomas Telford: London, UK, 1997.
31. Emery, J.J. Slag Utilization in Pavement Construction. In *Extending Aggregate Resources (ASTM Special Technical Publication 774)*; American Society for Testing and Materials: Philadelphia, PA, USA, 1982.
32. Jost, K.H.; Ziemer, B. Relations between the crystal structures of calcium silicates and their reactivity against water. *Cem. Concr. Res.* **1984**, *14*, 177–184. [CrossRef]
33. Mahieux, P.Y.; Aubert, J.E.; Escadeillas, G.; Measson, M. Quantification of hydraulic phase contained in a basic oxygen furnace slag. *J. Mater. Civ. Eng.* **2014**, *26*, 593–598. [CrossRef]
34. Mahoutian, M.; Shao, Y.; Mucci, A.; Fournier, B. Carbonation and hydration behavior of EAF and BOF steel slag binders. *Mater. Struct.* **2015**, *48*, 3075–3085. [CrossRef]
35. Adesanya, E.; Sreenivasan, H.; Kantola, A.M.; Telkki, V.-V.; Ohenoja, K.; Kinnunen, P.; Illikainen, M. Ladle slag cement–Characterization of hydration and conversion. *Constr. Build. Mater.* **2018**, *193*, 128–134. [CrossRef]
36. Choi, S.; Kim, J.-M.; Han, D.; Kim, J.-H. Hydration properties of ladle furnace slag powder rapidly cooled by air. *Constr. Build. Mater.* **2016**, *113*, 682–690. [CrossRef]
37. Rashad, A.M. A synopsis manual about recycling steel slag as a cementitious material. *J. Mater. Res. Technol.* **2019**, *8*, 4940–4955. [CrossRef]

38. Wang, Y.; Suraneni, P. Experimental methods to determine the feasibility of steel slags as supplementary cementitious materials. *Constr. Build. Mater.* **2019**, *204*, 458–467. [CrossRef]
39. Duda, A. Hydraulic reactions of LD steelwork slags. *Cem. Concr. Res.* **1989**, *19*, 793–801. [CrossRef]
40. Adesanya, E.; Ohenoja, K.; Kinnunen, P.; Illikainen, M. Properties and durability of alkali-activated ladle slag. *Mater. Struct.* **2017**, *50*, 255. [CrossRef]
41. Adesanya, E.; Ohenoja, K.; Kinnunen, P.; Illikainen, M. Alkali activation of ladle slag from steel-making process. *J. Sustain. Metall.* **2017**, *3*, 300–310. [CrossRef]
42. Nguyen, H.; Carvelli, V.; Adesanya, E.; Kinnunen, P.; Illikainen, M. High performance cementitious composite from alkali-activated ladle slag reinforced with polypropylene fibers. *Cem. Concr. Compos.* **2018**, *90*, 150–160. [CrossRef]
43. Češnovar, M.; Traven, K.; Horvat, B.; Ducman, V. The potential of ladle slag and electric arc furnace slag use in synthesizing alkali activated materials; the influence of curing on mechanical properties. *Materials* **2019**, *12*, 1173. [CrossRef] [PubMed]
44. Jing, W.; Jiang, J.; Ding, S.; Duan, P. Hydration and microstructure of steel slag as cementitious material and fine aggregate in mortar. *Molecules* **2020**, *25*, 4456. [CrossRef]
45. Salman, M.; Cizer, Ö.; Pontikes, Y.; Snellings, R.; Dijkman, J.; Sels, B.; Vandewalle, L.; Blanpain, B.; Van Balen, K. Alkali Activation of AOD Stainless Steel Slag under Steam Curing Conditions. *J. Am. Ceram. Soc.* **2015**, *98*, 3062–3074. [CrossRef]
46. Salman, M.; Cizer, Ö.; Pontikes, Y.; Vandewalle, L.; Blanpain, B.; Van Balen, K. Effect of curing temperatures on the alkali activation of crystalline continuous casting stainless steel slag. *Constr. Build. Mater.* **2014**, *71*, 308–316. [CrossRef]
47. Salman, M.; Cizer, Ö.; Pontikes, Y.; Snellings, R.; Vandewalle, L.; Blanpain, B.; Balen, K. Van Cementitious binders from activated stainless steel refining slag and the effect of alkali solutions. *J. Hazard. Mater.* **2015**, *286*, 211–219. [CrossRef]
48. Salman, M.; Cizer, Ö.; Pontikes, Y.; Snellings, R.; Vandewalle, L.; Blanpain, B.; Van Balen, K. Investigating the binding potential of continuous casting stainless steel slag by alkali activation. *Adv. Cem. Res.* **2014**, *26*, 256–270. [CrossRef]
49. Lizarazo-Marriaga, J.; Claisse, P.; Ganjian, E. Effect of steel slag and portland cement in the rate of hydration and strength of blast furnace slag pastes. *J. Mater. Civ. Eng.* **2011**, *23*, 153–160. [CrossRef]
50. Adolfsson, D.; Robinson, R.; Engström, F.; Björkman, B. Influence of mineralogy on the hydraulic properties of ladle slag. *Cem. Concr. Res.* **2011**, *41*, 865–871. [CrossRef]
51. Bell, F.G. Lime stabilization of clay minerals and soils. *Eng. Geol.* **1996**, *42*, 223–237. [CrossRef]
52. Prusinski, J.R.; Bhattacharja, S. Effectiveness of portland cement and lime in stabilizing clay soils. *Transp. Res. Rec.* **1999**, *1652*, 215–227. [CrossRef]
53. Zhao, H.; Liu, J.; Guo, J.; Zhao, C. Reexamination of lime stabilization mechanisms of expansive clay. *J. Mater. Civ. Eng.* **2015**, *27*, 04014108. [CrossRef]
54. Diamond, S.; Kinter, E.B. Mechanisms of soil-lime stabilization: An interpretive review. *Highw. Res. Rec.* **1965**, *92*, 83–102.
55. Jha, A.K.; Sivapullaiah, P.V. Lime stabilization of soil: A physico-chemical and micro-mechanistic perspective. *Indian Geotech. J.* **2020**, *50*, 339–347. [CrossRef]
56. Manso, J.M.; Polanco, J.A.; Losañez, M.; González, J.J. Durability of concrete made with EAF slag as aggregate. *Cem. Concr. Compos.* **2006**, *28*, 528–534. [CrossRef]
57. Rondi, L.; Bregoli, G.; Sorlini, S.; Cominoli, L.; Collivignarelli, C.; Plizzari, G. Concrete with EAF steel slag as aggregate: A comprehensive technical and environmental characterisation. *Compos. Part B Eng.* **2016**, *90*, 195–202. [CrossRef]
58. De Domenico, D.; Faleschini, F.; Pellegrino, C.; Ricciardi, G. Structural behavior of RC beams containing EAF slag as recycled aggregate: Numerical versus experimental results. *Constr. Build. Mater.* **2018**, *171*, 321–337. [CrossRef]
59. Faleschini, F.; Santamaria, A.; Zanini, M.A.; San José, J.T.; Pellegrino, C. Bond between steel reinforcement bars and electric arc furnace slag concrete. *Mater. Struct.* **2017**, *50*, 170. [CrossRef]
60. Papayianni, I.; Anastasiou, E. Production of high-strength concrete using high volume of industrial by-products. *Constr. Build. Mater.* **2010**, *24*, 1412–1417. [CrossRef]

61. Qasrawi, H.; Shalabi, F.; Asi, I. Use of low CaO unprocessed steel slag in concrete as fine aggregate. *Constr. Build. Mater.* **2009**, *23*, 1118–1125. [CrossRef]
62. Faleschini, F.; Alejandro Fernández-Ruíz, M.; Zanini, M.A.; Brunelli, K.; Pellegrino, C.; Hernández-Montes, E. High performance concrete with electric arc furnace slag as aggregate: Mechanical and durability properties. *Constr. Build. Mater.* **2015**, *101*, 113–121. [CrossRef]
63. Adegoloye, G.; Beaucour, A.-L.; Ortola, S.; Noumowé, A. Concretes made of EAF slag and AOD slag aggregates from stainless steel process: Mechanical properties and durability. *Constr. Build. Mater.* **2015**, *76*, 313–321. [CrossRef]
64. Faleschini, F.; Hofer, L.; Zanini, M.A.; dalla Benetta, M.; Pellegrino, C. Experimental behavior of beam-column joints made with EAF concrete under cyclic loading. *Eng. Struct.* **2017**, *139*, 81–95. [CrossRef]
65. Roy, S.; Miura, T.; Nakamura, H.; Yamamoto, Y. Investigation of fresh behaviors and mechanical properties of concrete produced by air granulated spherical shaped EAF slag fine aggregate. *Trans. Jpn. Concr. Inst.* **2018**, *40*, 1947–1952.
66. Arribas, I.; Santamaría, A.; Ruiz, E.; Ortega-López, V.; Manso, J.M. Electric arc furnace slag and its use in hydraulic concrete. *Constr. Build. Mater.* **2015**, *90*, 68–79. [CrossRef]
67. Monosi, S.; Ruello, M.L.; Sani, D. Electric arc furnace slag as natural aggregate replacement in concrete production. *Cem. Concr. Compos.* **2016**, *66*, 66–72. [CrossRef]
68. Polanco, J.A.; Manso, J.M.; Setién, J.; González, J.J. Strength and durability of concrete made with electric steelmaking slag. *ACI Mater. J.* **2011**, *108*, 196–203. [CrossRef]
69. Fuente-Alonso, J.A.; Ortega-López, V.; Skaf, M.; Aragón, Á.; San-José, J.T. Performance of fiber-reinforced EAF slag concrete for use in pavements. *Constr. Build. Mater.* **2017**, *149*, 629–638. [CrossRef]
70. Maslehuddin, M.; Sharif, A.M.; Shameem, M.; Ibrahim, M.; Barry, M.S. Comparison of properties of steel slag and crushed limestone aggregate concretes. *Constr. Build. Mater.* **2003**, *17*, 105–112. [CrossRef]
71. Papayianni, I.; Anastasiou, E. Concrete incorporating high-calcium fly ash and EAF slag aggregates. *Mag. Concr. Res.* **2011**, *63*, 597–604. [CrossRef]
72. Sersale, R.; Amicarelli, V.; Frigione, G.; Ubbriaco, P. A study on the utilization of an Italian steel slag. In Proceedings of the 8th International Congress on the Chemistry of Cement, Rio de Janeiro, Brazil, 22–27 September 1986; Volume 1, pp. 194–198.
73. Alizadeh, R.; Chini, M.; Ghods, P.; Hoseini, M.; Montazer, S.; Shekarchi, M. Utilization of electric arc furnace slag as aggregates in concrete–environmental issue. In Proceedings of the 6th CANMET/ACI International Conference on Recent Advances in Concrete Technology, Bucharest, Romania, 8–11 June 2003; pp. 451–464.
74. Coppola, L.; Lorenzi, S.; Buoso, A. Electric arc furnace granulated slag as a partial replacement of natural aggregates for concrete production. In Proceedings of the 2nd International Conference on Sustainable Construction Materials and Technologies, Ancona, Italy, 28–30 June 2010; pp. 1–9.
75. Etxeberria, M.; Pacheco, C.; Meneses, J.M.; Berridi, I. Properties of concrete using metallurgical industrial by-products as aggregates. *Constr. Build. Mater.* **2010**, *24*, 1594–1600. [CrossRef]
76. Abu-Eishah, S.I.; El-Dieb, A.S.; Bedir, M.S. Performance of concrete mixtures made with electric arc furnace (EAF) steel slag aggregate produced in the Arabian Gulf region. *Constr. Build. Mater.* **2012**, *34*, 249–256. [CrossRef]
77. Anastasiou, E.; Filikas, K.G.; Stefanidou, M. Utilization of fine recycled aggregates in concrete with fly ash and steel slag. *Constr. Build. Mater.* **2014**, *50*, 154–161. [CrossRef]
78. Qasrawi, H. Use of relatively high Fe2O3 steel slag as coarse aggregate in concrete. *ACI Mater. J.* **2012**, *109*. [CrossRef]
79. Moon, H.Y.; Yoo, J.H.; Kim, S.S. A fundamental study on the steel slag aggregate for concrete. *Geosystem Eng.* **2002**, *5*, 38–45. [CrossRef]
80. Yi, H.; Xu, G.; Cheng, H.; Wang, J.; Wan, Y.; Chen, H. An overview of utilization of steel slag. *Procedia Environ. Sci.* **2012**, *16*, 791–801. [CrossRef]
81. Jiang, Y.; Ling, T.-C.; Shi, C.; Pan, S.-Y. Characteristics of steel slags and their use in cement and concrete—A review. *Resour. Conserv. Recycl.* **2018**, *136*, 187–197. [CrossRef]
82. Qasrawi, H. Hardened properties of green self-consolidating concrete made with steel slag coarse aggregates under hot conditions. *ACI Mater. J.* **2020**, *117*, 107–118. [CrossRef]

83. Roy, S.; Miura, T.; Nakamura, H.; Yamamoto, Y. High temperature influence on concrete produced by spherical shaped EAF slag fine aggregate—Physical and mechanical properties. *Constr. Build. Mater.* **2020**, *231*, 117153. [CrossRef]
84. Rooholamini, H.; Sedghi, R.; Ghobadipour, B.; Adresi, M. Effect of electric arc furnace steel slag on the mechanical and fracture properties of roller-compacted concrete. *Constr. Build. Mater.* **2019**, *211*, 88–98. [CrossRef]
85. Pellegrino, C.; Faleschini, F. Experimental behavior of reinforced concrete beams with electric arc furnace slag as recycled aggregate. *ACI Mater. J.* **2013**, *110*, 197–205. [CrossRef]
86. Pellegrino, C.; Cavagnis, P.; Faleschini, F.; Brunelli, K. Properties of concretes with Black/Oxidizing Electric Arc Furnace slag aggregate. *Cem. Concr. Compos.* **2013**, *37*, 232–240. [CrossRef]
87. San-José, J.T.; Vegas, I.; Arribas, I.; Marcos, I. The performance of steel-making slag concretes in the hardened state. *Mater. Des.* **2014**, *60*, 612–619. [CrossRef]
88. Kim, S.W.; Lee, Y.J.; Kim, K.H. Flexural behavior of reinforced concrete beams with electric arc furnace slag aggregates. *J. Asian Archit. Build. Eng.* **2012**, *11*, 133–138. [CrossRef]
89. Vàzquez Ramonich, E.; Barra, M. Reactivity and expansion of electric arc furnace slag in their application in construction. *Mater. Constr.* **2001**, *51*, 137–148. [CrossRef]
90. Pellegrino, C.; Gaddo, V. Mechanical and durability characteristics of concrete containing EAF slag as aggregate. *Cem. Concr. Compos.* **2009**, *31*, 663–671. [CrossRef]
91. Ducman, V.; Mladenovič, A. The potential use of steel slag in refractory concrete. *Mater. Charact.* **2011**, *62*, 716–723. [CrossRef]
92. Ameri, M.; Shahabishahmiri, H.; Kazemzadehazad, S. Evaluation of the use of steel slag in concrete. In Proceedings of the 25th ARRB Conference, Perth, Australia, 25–28 September 2012.
93. Rezaul, R.M.; Atahar, R.; Bin Tasnim, T.; Kurny, A.S.W.; Momtaz, R.; Gulshan, F. Feasibility study of Bangladeshi electric arc furnace steel slag as an alternative for conventional fine aggregate. *AIP Conf. Proc.* **2018**, *1980*, 030028. [CrossRef]
94. Santamaría, A.; Orbe, A.; Losañez, M.M.; Skaf, M.; Ortega-Lopez, V.; González, J.J. Self-compacting concrete incorporating electric arc-furnace steelmaking slag as aggregate. *Mater. Des.* **2017**, *115*, 179–193. [CrossRef]
95. Muhmood, L.; Vitta, S.; Venkateswaran, D. Cementitious and pozzolanic behavior of electric arc furnace steel slags. *Cem. Concr. Res.* **2009**, *39*, 102–109. [CrossRef]
96. Lam, M.N.-T.; Jaritngam, S.; Le, D.-H. Roller-compacted concrete pavement made of Electric Arc Furnace slag aggregate: Mix design and mechanical properties. *Constr. Build. Mater.* **2017**, *154*, 482–495. [CrossRef]
97. Sosa, I.; Thomas, C.; Polanco, J.A.; Setién, J.; Tamayo, P. High performance self-compacting concrete with electric arc furnace slag aggregate and cupola slag powder. *Appl. Sci.* **2020**, *10*, 773. [CrossRef]
98. Tamayo, P.; Pacheco, J.; Thomas, C.; de Brito, J.; Rico, J. Mechanical and durability properties of concrete with coarse recycled aggregate produced with electric arc furnace slag concrete. *Appl. Sci.* **2020**, *10*, 216. [CrossRef]
99. Manso, J.M.; Gonzalez, J.J.; Polanco, J.A. Electric arc furnace slag in concrete. *J. Mater. Civ. Eng.* **2004**, *16*, 639–645. [CrossRef]
100. Chunlin, L.; Kunpeng, Z.; Depeng, C. Possibility of concrete prepared with steel slag as fine and coarse aggregates: A preliminary study. *Procedia Eng.* **2011**, *24*, 412–416. [CrossRef]
101. Al-Negheimish, A.I.; Al-Sugair, F.H.; Al-Zaid, R.Z. Utilization of local steelmaking slag in concrete. *J. King Saud Univ. Sci.* **1997**, *9*, 39–54. [CrossRef]
102. Santamaría, A.; Orbe, A.; San José, J.T.; González, J.J. A study on the durability of structural concrete incorporating electric steelmaking slags. *Constr. Build. Mater.* **2018**, *161*, 94–111. [CrossRef]
103. Kim, S.W.; Lee, Y.J.; Lee, Y.H.; Kim, K.H. Flexural performance of reinforced high-strength concrete beams with EAF oxidizing slag aggregates. *J. Asian Archit. Build. Eng.* **2016**, *15*, 589–596. [CrossRef]
104. Ortega-López, V.; Fuente-Alonso, J.A.; Santamaría, A.; San-José, J.T.; Aragón, Á. Durability studies on fiber-reinforced EAF slag concrete for pavements. *Constr. Build. Mater.* **2018**, *163*, 471–481. [CrossRef]
105. Madej, J.; Števula, L.; Slovák, K. Investigation of industrial by-products considered for use as concrete aggregates. In *Concrete for Environment Enhancement and Protection*; Dhir, R.K., Dyer, T.D., Eds.; E&FN Spon: London, UK, 1996; pp. 99–108.
106. Frıías Rojas, M.; Sánchez de Rojas, M.I. Chemical assessment of the electric arc furnace slag as construction material: Expansive compounds. *Cem. Concr. Res.* **2004**, *34*, 1881–1888. [CrossRef]

107. Luxán, M.P.; Sotolongo, R.; Dorrego, F.; Herrero, E. Characteristics of the slags produced in the fusion of scrap steel by electric arc furnace. *Cem. Concr. Res.* **2000**, *30*, 517–519. [CrossRef]
108. Netinger, I.; Rukavina, M.J.; Mladenovič, A. Improvement of post-fire properties of concrete with steel slag aggregate. *Procedia Eng.* **2013**, *62*, 745–753. [CrossRef]
109. Qasrawi, H. Fresh properties of green SCC made with recycled steel slag coarse aggregate under normal and hot weather. *J. Clean. Prod.* **2018**, *204*, 980–991. [CrossRef]
110. Frías Rojas, M.; Sánchez De Rojas, M.I.; Uría, A. Study of the instability of black slags from electric arc furnace steel industry. *Mater. Constr.* **2002**, *52*, 79–83. [CrossRef]
111. Netinger, I.; Bjegović, D.; Vrhovac, G. Utilisation of steel slag as an aggregate in concrete. *Mater. Struct.* **2011**, *44*, 1565–1575. [CrossRef]
112. Koh, T.; Moon, S.-W.; Jung, H.; Jeong, Y.; Pyo, S. Feasibility Study on the Application of Basic Oxygen Furnace (BOF) Steel Slag for Railway Ballast Material. *Sustainability* **2018**, *10*, 284. [CrossRef]
113. Wang, G.W. Properties and Utilization of Steel Slag in Engineering Applications. Ph.D. Thesis, University of Wollongong, Wollongong, Australia, 1992.
114. Pang, B.; Zhou, Z.; Xu, H. Utilization of carbonated and granulated steel slag aggregate in concrete. *Constr. Build. Mater.* **2015**, *84*, 454–467. [CrossRef]
115. Zareei, S.A.; Ameri, F.; Bahrami, N.; Shoaei, P.; Moosaei, H.R.; Salemi, N. Performance of sustainable high strength concrete with basic oxygen steel-making (BOS) slag and nano-silica. *J. Build. Eng.* **2019**, *25*, 100791. [CrossRef]
116. Ding, Y.-C.; Cheng, T.-W.; Liu, P.-C.; Lee, W.-H. Study on the treatment of BOF slag to replace fine aggregate in concrete. *Constr. Build. Mater.* **2017**, *146*, 644–651. [CrossRef]
117. Belhadj, E.; Diliberto, C.; Lecomte, A. Characterization and activation of Basic Oxygen Furnace slag. *Cem. Concr. Compos.* **2012**, *34*, 34–40. [CrossRef]
118. Reddy, A.S.; Pradhan, R.K.; Chandra, S. Utilization of Basic Oxygen Furnace (BOF) slag in the production of a hydraulic cement binder. *Int. J. Miner. Process.* **2006**, *79*, 98–105. [CrossRef]
119. Belhadj, E.; Diliberto, C.; Lecomte, A. Properties of hydraulic paste of basic oxygen furnace slag. *Cem. Concr. Compos.* **2014**, *45*, 15–21. [CrossRef]
120. Guo, Y.; Xie, J.; Zhao, J.; Zuo, K. Utilization of unprocessed steel slag as fine aggregate in normal- and high-strength concrete. *Constr. Build. Mater.* **2019**, *204*, 41–49. [CrossRef]
121. Ko, M.-S.; Chen, Y.-L.; Jiang, J.-H. Accelerated carbonation of basic oxygen furnace slag and the effects on its mechanical properties. *Constr. Build. Mater.* **2015**, *98*, 286–293. [CrossRef]
122. Sharma, S.; Singla, S. A Comparative Study on Effect of Basic Oxygen Furnace Slag and Iron Cutting Waste on Strength Properties of Concrete. *Int. J. Res. Eng. Technol.* **2015**, *4*, 478–482. [CrossRef]
123. Kawamura, M.; Torii, K.; Hasaba, S.; Nicho, N.; Oda, K. Applicability of basic oxygen furnace slag as a concrete aggregate. In *Fly Ash, Silica Fume, Slag and Other Mineral By-Products in Concrete*; ACI Special Publication 79; Malhotra, V.M., Ed.; American Concrete Institute: Detroit, MI, USA, 1983; Volume 79, pp. 1123–1142.
124. Bodor, M.; Santos, R.M.; Cristea, G.; Salman, M.; Cizer, Ö.; Iacobescu, R.I.; Chiang, Y.W.; van Balen, K.; Vlad, M.; van Gerven, T. Laboratory investigation of carbonated BOF slag used as partial replacement of natural aggregate in cement mortars. *Cem. Concr. Compos.* **2016**, *65*, 55–66. [CrossRef]
125. Lin, W.T.; Tsai, C.J.; Chen, J.; Liu, W. Feasibility and characterization mortar blended with high-amount basic oxygen furnace slag. *Materials* **2018**, *12*, 6. [CrossRef]
126. Lu, T.-H.; Chen, Y.-L.; Shih, P.-H.; Chang, J.-E. Use of basic oxygen furnace slag fines in the production of cementitious mortars and the effects on mortar expansion. *Constr. Build. Mater.* **2018**, *167*, 768–774. [CrossRef]
127. Tsai, C.-J.; Huang, R.; Lin, W.-T.; Wang, H.-N. Mechanical and cementitious characteristics of ground granulated blast furnace slag and basic oxygen furnace slag blended mortar. *Mater. Des.* **2014**, *60*, 267–273. [CrossRef]
128. Zhang, T.; Yu, Q.; Wei, J.; Li, J.; Zhang, P. Preparation of high performance blended cements and reclamation of iron concentrate from basic oxygen furnace steel slag. *Resour. Conserv. Recycl.* **2011**, *56*, 48–55. [CrossRef]
129. De Schutter, G.; Audenaert, K.; De Rouck, J. Full-scale static loading tests on concrete armour units with the incorporation of LD-slag. *Struct. Concr.* **2002**, *3*, 99–105. [CrossRef]
130. Sideris, K.K.; Tassos, C.; Chatzopoulos, A.; Manita, P. Mechanical characteristics and durability of self compacting concretes produced with ladle furnace slag. *Constr. Build. Mater.* **2018**, *170*, 660–667. [CrossRef]

131. Manso, J.M.; Losañez, M.; Polanco, J.A.; Gonzalez, J.J. Ladle furnace slag in construction. *J. Mater. Civ. Eng.* **2005**, *17*, 513–518. [CrossRef]
132. Anastasiou, E.K.; Papayianni, I.; Papachristoforou, M. Behavior of self compacting concrete containing ladle furnace slag and steel fiber reinforcement. *Mater. Des.* **2014**, *59*, 454–460. [CrossRef]
133. Iacobescu, R.I.; Koumpouri, D.; Pontikes, Y.; Saban, R.; Angelopoulos, G.N. Valorisation of electric arc furnace steel slag as raw material for low energy belite cements. *J. Hazard. Mater.* **2011**, *196*, 287–294. [CrossRef]
134. Rodriguez, Á.; Manso, J.M.; Aragón, Á.; Gonzalez, J.J. Strength and workability of masonry mortars manufactured with ladle furnace slag. *Resour. Conserv. Recycl.* **2009**, *53*, 645–651. [CrossRef]
135. Monkman, S.; Shao, Y.; Shi, C. Carbonated ladle slag fines for carbon uptake and sand substitute. *J. Mater. Civ. Eng.* **2009**, *21*, 657–665. [CrossRef]
136. Wang, G. Determination of the expansion force of coarse steel slag aggregate. *Constr. Build. Mater.* **2010**, *24*, 1961–1966. [CrossRef]
137. Pang, B.; Zhou, Z.; Cheng, X.; Du, P.; Xu, H. ITZ properties of concrete with carbonated steel slag aggregate in salty freeze-thaw environment. *Constr. Build. Mater.* **2016**, *114*, 162–171. [CrossRef]
138. Diao, Z.K.; Pan, Z.H.; Ma, J.; Gao, Z.; Qiu, T. Experimental study on workability and compressive strength of self-compacting concrete with recycled aggregate of steel slag. *Build. Struct.* **2016**, *46*, 52–55.
139. Wang, Q.; Yan, P.; Mi, G. Effect of blended steel slag–GBFS mineral admixture on hydration and strength of cement. *Constr. Build. Mater.* **2012**, *35*, 8–14. [CrossRef]
140. Özkan, Ö.; Sarıbıyık, M. Alkali silica reaction of BOF and BFS wastes combination in cement. *J. Civ. Eng. Manag.* **2013**, *19*, 113–120. [CrossRef]
141. Moosberg-Bustnes, H. Steel-Slag As Filler Material in Concrete. In *VII International Conference on Molten Slags Fluxes and Salts*; The South African Institute of Mining and Metallurgy: Johannesburg, South Africa, 2004; pp. 385–391.
142. Sheen, Y.-N.; Wang, H.-Y.; Sun, T.-H. Properties of green concrete containing stainless steel oxidizing slag resource materials. *Constr. Build. Mater.* **2014**, *50*, 22–27. [CrossRef]
143. Sheen, Y.-N.; Wang, H.-Y.; Sun, T.-H. A study of engineering properties of cement mortar with stainless steel oxidizing slag and reducing slag resource materials. *Constr. Build. Mater.* **2013**, *40*, 239–245. [CrossRef]
144. Gupta, T.; Sachdeva, S.N. Laboratory investigation and modeling of concrete pavements containing AOD steel slag. *Cem. Concr. Res.* **2019**, *124*, 105808. [CrossRef]
145. Moon, E.-J.; Choi, Y.C. Development of carbon-capture binder using stainless steel argon oxygen decarburization slag activated by carbonation. *J. Clean. Prod.* **2018**, *180*, 642–654. [CrossRef]
146. Salman, M.; Cizer, Ö.; Pontikes, Y.; Santos, R.M.; Snellings, R.; Vandewalle, L.; Blanpain, B.; Van Balen, K. Effect of accelerated carbonation on AOD stainless steel slag for its valorisation as a CO_2-sequestering construction material. *Chem. Eng. J.* **2014**, *246*, 39–52. [CrossRef]
147. Saxena, S.; Tembhurkar, A.R. Impact of use of steel slag as coarse aggregate and wastewater on fresh and hardened properties of concrete. *Constr. Build. Mater.* **2018**, *165*, 126–137. [CrossRef]
148. Devi, V.S.; Gnanavel, B.K. Properties of concrete manufactured using steel slag. *Procedia Eng.* **2014**, *97*, 95–104. [CrossRef]
149. Nadeem, M.; Pofale, A.D. Experimental investigation of using slag as an alternative to normal aggregates (coarse and fine) in concrete. *Int. J. Civ. Struct. Eng.* **2012**, *3*, 117–127. [CrossRef]
150. Montgomery, D.G.; Wang, G. Instant-chilled steel slag aggregate in concrete—Fracture related properties. *Cem. Concr. Res.* **1992**, *22*, 755–760. [CrossRef]
151. Montgomery, D.G.; Wang, G. Instant-chilled steel slag aggregate in concrete—Strength related properties. *Cem. Concr. Res.* **1991**, *21*, 1083–1091. [CrossRef]
152. Mo, L.; Zhang, F.; Deng, M.; Jin, F.; Al-Tabbaa, A.; Wang, A. Accelerated carbonation and performance of concrete made with steel slag as binding materials and aggregates. *Cem. Concr. Compos.* **2017**, *83*, 138–145. [CrossRef]
153. Mishra, B.K.; Bharosh, R. Evaluation strength and durability characteristic of concrete use steel slag. *Int. J. Adv. Res. Ideas Innov. Technol.* **2018**, *4*, V4I5–V1376.
154. Yuji, W. The effect of bond characteristics between steel slag fine aggregate and cement paste on mechanical properties of concrete and mortar. *Mater. Res. Soc. Symp. Proc.* **1987**, *114*, 49–54. [CrossRef]
155. Akinmusuru, J.O. Potential beneficial uses of steel slag wastes for civil engineering purposes. *Resour. Conserv. Recycl.* **1991**, *5*, 73–80. [CrossRef]

156. Beshr, H.; Almusallam, A.A.; Maslehuddin, M. Effect of coarse aggregate quality on the mechanical properties of high strength concrete. *Constr. Build. Mater.* **2003**, *17*, 97–103. [CrossRef]
157. Almusallam, A.A.; Beshr, H.; Maslehuddin, M.; Al-Amoudi, O.S.B. Effect of silica fume on the mechanical properties of low quality coarse aggregate concrete. *Cem. Concr. Compos.* **2004**, *26*, 891–900. [CrossRef]
158. Mohammed, K.J.; Abbas, F.O.; Abbas, M.O. Using of steel slag in modification of concrete properties. *Eng. Technol. J.* **2009**, *27*, 1711–1720.
159. Qasrawi, H. The use of steel slag aggregate to enhance the mechanical properties of recycled aggregate concrete and retain the environment. *Constr. Build. Mater.* **2014**, *54*, 298–304. [CrossRef]
160. Qasrawi, H.; Shalabi, F.; Asi, I. Effect of unprocessed steel slag on the strength of concrete when used as fine aggregate. In *Design and Sustainability of Structural Concrete in the Middle East with Emphasis on High-Rise Buildings*; El-Hawary, M.M., Al-Mutairi, N., Rahal, K.N., Kamal, H., Eds.; American Concrete Institute Kuwait Chapter: Kuwait City, Kuwait, 2007; pp. 227–237.
161. Tarawneh, S.A.; Gharaibeh, E.S.; Saraireh, F.M. Effect of using steel slag aggregate on mechanical properties of concrete. *Am. J. Appl. Sci.* **2014**, *11*, 700. [CrossRef]
162. Guo, Y.; Xie, J.; Zheng, W.; Li, J. Effects of steel slag as fine aggregate on static and impact behaviours of concrete. *Constr. Build. Mater.* **2018**, *192*, 194–201. [CrossRef]
163. Mathew, P.; Stephen, L.; George, J. Steel Slag ingredient for concrete pavement. *Int. J. Innov. Res. Sci. Eng. Technol.* **2013**, *2*, 710–714.
164. Sezer, G.İ.; Gülderen, M. Usage of steel slag in concrete as fine and/or coarse aggregate. *Indian J. Eng. Mater. Sci.* **2015**, *22*, 339–344.
165. Patel, J.P. Broader Use of Steel Slag Aggregates in Concrete. M.S. Thesis, Cleveland State University, Cleveland, OH, USA, 2008.
166. Vasanthi, P. Flexural behaviour of reinforced concrete slabs using steel slag as coarse aggregate replacement. *Int. J. Res. Eng. Technol.* **2014**, *3*, 141–146.
167. Wang, Q.; Yang, J.; Yan, P. Cementitious properties of super-fine steel slag. *Powder Technol.* **2013**, *245*, 35–39. [CrossRef]
168. Wang, Q.; Yan, P.; Yang, J.; Zhang, B. Influence of steel slag on mechanical properties and durability of concrete. *Constr. Build. Mater.* **2013**, *47*, 1414–1420. [CrossRef]
169. Mo, L.; Yang, S.; Huang, B.; Xu, L.; Feng, S.; Deng, M. Preparation, microstructure and property of carbonated artificial steel slag aggregate used in concrete. *Cem. Concr. Compos.* **2020**, *113*, 103715. [CrossRef]
170. Tripathi, B.; Misra, A.; Chaudhary, S. Strength and abrasion characteristics of ISF slag concrete. *J. Mater. Civ. Eng.* **2013**, *25*, 1611–1618. [CrossRef]
171. Maruthachalam, V.; Palanisamy, M. High performance concrete with steel slag aggregate. *Građevinar* **2014**, *7*, 605–612. [CrossRef]
172. Abd AlRahman, D.Y.A. *The Use of Steel Slag in Manufacturing of Portland Cement*; Sudan University of Sciences and Technology: Khartoum, Sudan, 2019.
173. Yu, X.; Tao, Z.; Song, T.-Y.; Pan, Z. Performance of concrete made with steel slag and waste glass. *Constr. Build. Mater.* **2016**, *114*, 737–746. [CrossRef]
174. Bosela, P.; Delatte, N.; Obratil, R.; Patel, A. Fresh and hardened properties of paving concrete with steel slag aggregate. In Proceedings of the 9th International Conference on Concrete Pavements, International Society for Concrete Pavements, San Francisco, CA, USA, 17–21 August 2008; pp. 836–853.
175. Li, Y.; Yao, Y.; Wang, L. Recycling of industrial waste and performance of steel slag green concrete. *J. Cent. South Univ. Technol.* **2009**, *16*, 768. [CrossRef]
176. Khan, M.S.H.; Castel, A.; Akbarnezhad, A.; Foster, S.J.; Smith, M. Utilisation of steel furnace slag coarse aggregate in a low calcium fly ash geopolymer concrete. *Cem. Concr. Res.* **2016**, *89*, 220–229. [CrossRef]
177. Hu, S.; Wang, H.; Zhang, G.; Ding, Q. Bonding and abrasion resistance of geopolymeric repair material made with steel slag. *Cem. Concr. Compos.* **2008**, *30*, 239–244. [CrossRef]
178. Niklioć, I.; Marković, S.; Janković-Častvan, I.; Radmilović, V.V.; Karanović, L.; Babić, B.; Radmilović, V.R. Modification of mechanical and thermal properties of fly ash-based geopolymer by the incorporation of steel slag. *Mater. Lett.* **2016**, *176*, 301–305. [CrossRef]
179. Al-Rawi, S.; Taysi, N. Performance of self-compacting geopolymer concrete with and without GGBFS and steel fiber. *Adv. Concr. Constr.* **2018**, *6*, 323–344. [CrossRef]

180. Mastali, M.; Alzaza, A.; Shaad, K.M.; Kinnunen, P.; Abdollahnejad, Z.; Woof, B.; Illikainen, M. Using carbonated BOF slag aggregates in alkali-activated concretes. *Materials* **2019**, *12*, 1288. [CrossRef]
181. Natali Murri, A.; Rickard, W.D.A.; Bignozzi, M.C.; van Riessen, A. High temperature behaviour of ambient cured alkali-activated materials based on ladle slag. *Cem. Concr. Res.* **2013**, *43*, 51–61. [CrossRef]
182. Lancellotti, I.; Ponzoni, C.; Bignozzi, M.C.; Barbieri, L.; Leonelli, C. Incinerator bottom ash and ladle slag for geopolymers preparation. *Waste Biomass Valor.* **2014**, *5*, 393–401. [CrossRef]
183. Bignozzi, M.C.; Manzi, S.; Lancellotti, I.; Kamseu, E.; Barbieri, L.; Leonelli, C. Mix-design and characterization of alkali activated materials based on metakaolin and ladle slag. *Appl. Clay Sci.* **2013**, *73*, 78–85. [CrossRef]
184. Castel, A.; Khan, M.; Mahmood, A.; Foster, S. Utilization of steel furnace aggregate in geopolymer concrete for wave-breaker application. In *Durability and Sustainability of Concrete Structures*; Falikman, V., Realfonzo, R., Coppola, L., Hàjek, P., Riva, P., Eds.; American Concrete Institute: Farmington Hills, MI, USA, 2018; Volume 326, pp. 25.1–25.10.
185. Ashadi, H.W.; Aprilando, B.A.; Astutiningsih, S. Effects of steel slag substitution in geopolymer concrete on compressive strength and corrosion rate of steel reinforcement in seawater and an acid rain environment. *Int. J. Technol.* **2015**, *6*, 227–235. [CrossRef]
186. Omar, O.M.; Heniegal, A.M.; Abd Elhameed, G.D.; Mohamadien, H.A. Effect of local steel slag as a coarse aggregate on properties of fly-ash based geopolymer concrete. *Int. J. Civ. Environ. Struct. Constr. Archit. Eng.* **2015**, *9*, 1464–1472.
187. Guo, X.; Pan, X. Mechanical properties and mechanisms of fiber reinforced fly ash–steel slag based geopolymer mortar. *Constr. Build. Mater.* **2018**, *179*, 633–641. [CrossRef]
188. Bai, T.; Song, Z.-G.; Wu, Y.-G.; Hu, X.-D.; Bai, H. Influence of steel slag on the mechanical properties and curing time of metakaolin geopolymer. *Ceram. Int.* **2018**, *44*, 15706–15713. [CrossRef]
189. Biskri, Y.; Achoura, D.; Chelghoum, N.; Mouret, M. Mechanical and durability characteristics of High Performance Concrete containing steel slag and crystalized slag as aggregates. *Constr. Build. Mater.* **2017**, *150*, 167–178. [CrossRef]
190. You, N.; Li, B.; Cao, R.; Shi, J.; Chen, C.; Zhang, Y. The influence of steel slag and ferronickel slag on the properties of alkali-activated slag mortar. *Constr. Build. Mater.* **2019**, *227*, 116614. [CrossRef]
191. Mahmood, A.H.; Foster, S.J.; Castel, A. Development of high-density geopolymer concrete with steel furnace slag aggregate for coastal protection structures. *Constr. Build. Mater.* **2020**, *248*, 118681. [CrossRef]
192. Palankar, N.; Ravi Shankar, A.U.; Mithun, B.M. Investigations on Alkali-Activated Slag/Fly Ash Concrete with steel slag coarse aggregate for pavement structures. *Int. J. Pavement Eng.* **2017**, *18*, 500–512. [CrossRef]
193. Palankar, N.; Ravi Shankar, A.U.; Mithun, B.M. Durability studies on eco-friendly concrete mixes incorporating steel slag as coarse aggregates. *J. Clean. Prod.* **2016**, *129*, 437–448. [CrossRef]
194. Van Dao, D.; Trinh, S.H.; Ly, H.-B.; Pham, B.T. Prediction of compressive strength of geopolymer concrete using entirely steel slag aggregates: Novel hybrid artificial intelligence approaches. *Appl. Sci.* **2019**, *9*, 1113. [CrossRef]
195. Roslan, N.H.; Ismail, M.; Abdul-Majid, Z.; Ghoreishiamiri, S.; Muhammad, B. Performance of steel slag and steel sludge in concrete. *Constr. Build. Mater.* **2016**, *104*, 16–24. [CrossRef]
196. Kanagawa, A.; Kuwayama, T. The improvement of soft clayey soil utilizing reducing slag produced from electric arc furnace. *Denki-Seiko* **1997**, *68*, 261–267. [CrossRef]
197. Shen, W.; Zhou, M.; Ma, W.; Hu, J.; Cai, Z. Investigation on the application of steel slag–fly ash–phosphogypsum solidified material as road base material. *J. Hazard. Mater.* **2009**, *164*, 99–104. [CrossRef]
198. Barišić, I.; Dimter, S.; Rukavina, T. Strength properties of steel slag stabilized mixes. *Compos. Part B Eng.* **2014**, *58*, 386–391. [CrossRef]
199. Barra, M.; Ramonich, E.V.; Munoz, M.A. Stabilization of soils with steel slag and cement for application in rural and low traffic roads. In *Beneficial Use of Recycled Materials in Transportation Applications*; Eighmy, T.T., Ed.; Air and Waste Management Association: Sewickley, PA, USA, 2003; pp. 423–432. ISBN 0923204490.
200. Akinwumi, I. Soil modification by the application of steel slag. *Period. Polytech. Civ. Eng.* **2014**, *58*, 371–377. [CrossRef]
201. Cheng, T.; Hu, R.; Xu, W.; Zhang, Y. Mechanical characterizations of oxidizing steel slag soil and application. *Period. Polytech. Civ. Eng.* **2017**, *61*, 815–823. [CrossRef]
202. Lee, J.-Y.; Choi, J.-S.; Yuan, T.-F.; Yoon, Y.-S.; Mitchell, D. Comparing properties of concrete containing electric arc furnace slag and granulated blast furnace slag. *Materials* **2019**, *12*, 1371. [CrossRef]

203. Conjeaud, M.; George, C.M.; Sorrentino, F.P. A new steel slag for cement manufacture: Mineralogy and hydraulicity. *Cem. Concr. Res.* **1981**, *11*, 85–102. [CrossRef]
204. Guo, X.; Shi, H. Utilization of steel slag powder as a combined admixture with ground granulated blast-furnace slag in cement based materials. *J. Mater. Civ. Eng.* **2013**, *25*, 1990–1993. [CrossRef]
205. Alanyali, H.; Çöl, M.; Yilmaz, M.; Karagöz, Ş. Concrete produced by steel-making slag (basic oxygen furnace) addition in portland cement. *Int. J. Appl. Ceram. Technol.* **2009**, *6*, 736–748. [CrossRef]
206. Carvalho, S.Z.; Vernilli, F.; Almeida, B.; Demarco, M.; Silva, S.N. The recycling effect of BOF slag in the portland cement properties. *Resour. Conserv. Recycl.* **2017**, *127*, 216–220. [CrossRef]
207. Guo, H.; Yin, S.; Yu, Q.; Yang, X.; Huang, H.; Yang, Y.; Gao, F. Iron recovery and active residue production from basic oxygen furnace (BOF) slag for supplementary cementitious materials. *Resour. Conserv. Recycl.* **2018**, *129*, 209–218. [CrossRef]
208. Poh, H.Y.; Ghataora, G.S.; Ghazireh, N. Soil stabilization using basic oxygen steel slag fines. *J. Mater. Civ. Eng.* **2006**, *18*, 229–240. [CrossRef]
209. Goodarzi, A.R.; Salimi, M. Stabilization treatment of a dispersive clayey soil using granulated blast furnace slag and basic oxygen furnace slag. *Appl. Clay Sci.* **2015**, *108*, 61–69. [CrossRef]
210. Kang, G.; Cikmit, A.A.; Tsuchida, T.; Honda, H.; Kim, Y. Strength development and microstructural characteristics of soft dredged clay stabilized with basic oxygen furnace steel slag. *Constr. Build. Mater.* **2019**, *203*, 501–513. [CrossRef]
211. Diniz, D.H.; de Carvalho, J.M.F.; Mendes, J.C.; Peixoto, R.A.F. Blast oxygen furnace slag as chemical soil stabilizer for use in roads. *J. Mater. Civ. Eng.* **2017**, *29*, 4017118. [CrossRef]
212. Mirzaeifar, H.; Abdi, M.R. Stabilizing clays using basic oxygen steel slag (BOS). In *Recent Research, Advances and Execution Aspects of Ground Improvement Works*; Denies, N., Huybrechts, N., Eds.; International Society for Soil Mechanics and Geotechnical Engineering: Brussels, Belgium, 2012; Volume II, pp. 403–410.
213. Shahbazi, M.; Rowshanzamir, M.; Abtahi, S.M.; Hejazi, S.M. Optimization of carpet waste fibers and steel slag particles to reinforce expansive soil using response surface methodology. *Appl. Clay Sci.* **2017**, *142*, 185–192. [CrossRef]
214. Akın Altun, İ.; Yılmaz, İ. Study on steel furnace slags with high MgO as additive in Portland cement. *Cem. Concr. Res.* **2002**, *32*, 1247–1249. [CrossRef]
215. Mahieux, P.-Y.; Aubert, J.-E.; Escadeillas, G. Utilization of weathered basic oxygen furnace slag in the production of hydraulic road binders. *Constr. Build. Mater.* **2009**, *23*, 742–747. [CrossRef]
216. Dongxue, L.; Xinhua, F.; Xuequan, W.; Mingshu, T. Durability study of steel slag cement. *Cem. Concr. Res.* **1997**, *27*, 983–987. [CrossRef]
217. Murphy, J.N.; Meadowcroft, T.R.; Barr, P. V Enhancement of the cementitious properties of steelmaking slag. *Can. Metall. Q.* **1997**, *36*, 315–331. [CrossRef]
218. Ortega-López, V.; Manso, J.M.; Cuesta, I.I.; González, J.J. The long-term accelerated expansion of various ladle-furnace basic slags and their soil-stabilization applications. *Constr. Build. Mater.* **2014**, *68*, 455–464. [CrossRef]
219. Manso, J.M.; Ortega-López, V.; Polanco, J.A.; Setién, J. The use of ladle furnace slag in soil stabilization. *Constr. Build. Mater.* **2013**, *40*, 126–134. [CrossRef]
220. Montenegro, J.M.; Celemín-Matachana, M.; Cañizal, J.; Setién, J. Ladle furnace slag in the construction of embankments: Expansive behavior. *J. Mater. Civ. Eng.* **2013**, *25*, 972–979. [CrossRef]
221. Yzenas, J.J. The utilization of steel furnace slag for soil stabilization. In *Ferrous Slag—Resource Development for an Environmentally Sustainable World*; EUROSLAG: Duisburg, Germany, 2010; pp. 359–368.
222. Brand, A.S.; Singhvi, P.; Fanijo, E.O.; Tutumluer, E. Stabilization of a clayey soil with ladle metallurgy furnace slag fines. *Materials* **2020**, *13*, 4251. [CrossRef] [PubMed]
223. Shi, C.; Hu, S. Cementitious properties of ladle slag fines under autoclave curing conditions. *Cem. Concr. Res.* **2003**, *33*, 1851–1856. [CrossRef]
224. Papayianni, I.; Anastasiou, E. Effect of granulometry on cementitious properties of ladle furnace slag. *Cem. Concr. Compos.* **2012**, *34*, 400–407. [CrossRef]
225. Papayianni, I.; Anastasiou, E. Optimization of ladle furnace slag for use as a supplementary cementing material. In *Measuring, Monitoring and Modeling Concrete Properties*; Konsta-Gdoutos, M.S., Ed.; Springer: Dordrecht, The Netherlands, 2006; pp. 411–417.

226. Rosales, J.; Cabrera, M.; Agrela, F. Effect of stainless steel slag waste as a replacement for cement in mortars. Mechanical and statistical study. *Constr. Build. Mater.* **2017**, *142*, 444–458. [CrossRef]
227. Xuequan, W.; Hong, Z.; Xinkai, H.; Husen, L. Study on steel slag and fly ash composite Portland cement. *Cem. Concr. Res.* **1999**, *29*, 1103–1106. [CrossRef]
228. Monshi, A.; Asgarani, M.K. Producing Portland cement from iron and steel slags and limestone. *Cem. Concr. Res.* **1999**, *29*, 1373–1377. [CrossRef]
229. Peng, Y.-C.; Hwang, C.-L. Carbon steel slag as cementitious material for self-consolidating concrete. *J. Zhejiang Univ. A* **2010**, *11*, 488–494. [CrossRef]
230. Chen, W.; Huo, Z.; Yang, Z. Study on the performance of green cement with large amount of steel slag addition. *IOP Conf. Ser. Earth Environ. Sci.* **2019**, *233*, 22015. [CrossRef]
231. Pamukcu, S.; Tuncan, A. Laboratory characterization of cement-stabilized iron-rich slag for reuse in transportation facilities. *Transp. Res. Rec.* **1993**, *1424*, 25.
232. Gu, X.; Yu, B.; Dong, Q.; Deng, Y. Application of secondary steel slag in subgrade: Performance evaluation and enhancement. *J. Clean. Prod.* **2018**, *181*, 102–108. [CrossRef]
233. Wu, J.; Liu, Q.; Deng, Y.; Yu, X.; Feng, Q.; Yan, C. Expansive soil modified by waste steel slag and its application in subbase layer of highways. *Soils Found.* **2019**, *59*, 955–965. [CrossRef]
234. Cheng, T.; Yan, K.Q. Mechanics properties of the lime-steel slag stabilized soil for pavement structures. *Adv. Mater. Res.* **2011**, *168–170*, 931–935. [CrossRef]
235. Chan, C.-M.; Mizutani, T.; Kikuchi, Y. Reusing dredged marine clay by solidification with steel slag: A study of compressive strength. *Int. J. Civ. Struct. Eng.* **2011**, *2*, 270–279.
236. Shalabi, F.I.; Asi, I.M.; Qasrawi, H.Y. Effect of by-product steel slag on the engineering properties of clay soils. *J. King Saud Univ. Eng. Sci.* **2017**, *29*, 394–399. [CrossRef]
237. Akinwumi, I.I.; Adeyeri, J.B.; Ejohwomu, O.A. Effects of steel slag addition on the plasticity, strength, and permeability of lateritic soil. In *ICSDEC 2012: Developing the Frontier of Sustainable Design, Engineering, and Construction*; Chong, W.K.O., Gong, J., Chang, J., Siddiqui, M.K., Eds.; American Society of Civil Engineers: Reston, VA, USA, 2013; pp. 457–464.
238. Ashango, A.A.; Patra, N.R. Behavior of expansive soil treated with steel slag, rice husk ash, and lime. *J. Mater. Civ. Eng.* **2016**, *28*, 6016008. [CrossRef]
239. Aldeeky, H.; Al Hattamleh, O. Experimental study on the utilization of fine steel slag on stabilizing high plastic subgrade soil. *Adv. Civ. Eng.* **2017**, *2017*. [CrossRef]
240. Liu, L.; Zhou, A.; Deng, Y.; Cui, Y.; Yu, Z.; Yu, C. Strength performance of cement/slag-based stabilized soft clays. *Constr. Build. Mater.* **2019**, *211*, 909–918. [CrossRef]
241. Zumrawi, M.M.E.; Babikir, A.A.-A.A. Laboratory study of steel slag used for stabilizing expansive soil. *Asian Eng. Rev.* **2017**, *4*, 1–6. [CrossRef]
242. Kourounis, S.; Tsivilis, S.; Tsakiridis, P.E.; Papadimitriou, G.D.; Tsibouki, Z. Properties and hydration of blended cements with steelmaking slag. *Cem. Concr. Res.* **2007**, *37*, 815–822. [CrossRef]
243. Tüfekçi, M.; Demirbaş, A.; Genç, H. Evaluation of steel furnace slags as cement additives. *Cem. Concr. Res.* **1997**, *27*, 1713–1717. [CrossRef]
244. Rai, A.; Prabakar, J.; Raju, C.B.; Morchalle, R.K. Metallurgical slag as a component in blended cement. *Constr. Build. Mater.* **2002**, *16*, 489–494. [CrossRef]
245. Qiang, W.; Mengxiao, S.; Jun, Y. Influence of classified steel slag with particle sizes smaller than 20 μm on the properties of cement and concrete. *Constr. Build. Mater.* **2016**, *123*, 601–610. [CrossRef]
246. Zhang, T.; Yu, Q.; Wei, J.; Li, J. Investigation on mechanical properties, durability and micro-structural development of steel slag blended cements. *J. Therm. Anal. Calorim.* **2012**, *110*, 633–639. [CrossRef]
247. Tsakiridis, P.E.; Papadimitriou, G.D.; Tsivilis, S.; Koroneos, C. Utilization of steel slag for Portland cement clinker production. *J. Hazard. Mater.* **2008**, *152*, 805–811. [CrossRef]
248. Liu, Q.D.; Sun, J.Y.; Han, Y. Research on performance of steel slag and porous cement concrete made by steel slag aggregate. *Adv. Mater. Res.* **2011**, *214*, 306–311. [CrossRef]
249. Yong-Feng, D.; Tong-Wei, Z.; Yu, Z.; Qian-Wen, L.; Qiong, W. Mechanical behaviour and microstructure of steel slag-based composite and its application for soft clay stabilisation. *Eur. J. Environ. Civ. Eng.* **2017**, 1–16. [CrossRef]
250. Sinha, A.K.; Havanagi, V.G.; Ranjan, A.; Mathur, S. Steel slag waste material for the construction of road. *Indian Highw.* **2013**, *41*, 15–22.

251. Coomarasamy, A.; Walzak, T.L. Effects of moisture on surface chemistry of steel slags and steel slag-asphalt paving mixes. *Transp. Res. Rec.* **1995**, *1492*, 85–95.
252. Wang, D.; Chang, J.; Ansari, W.S. The effects of carbonation and hydration on the mineralogy and microstructure of basic oxygen furnace slag products. *J. CO_2 Util.* **2019**, *34*, 87–98. [CrossRef]
253. Ghouleh, Z.; Guthrie, R.I.L.; Shao, Y. High-strength KOBM steel slag binder activated by carbonation. *Constr. Build. Mater.* **2015**, *99*, 175–183. [CrossRef]
254. Chen, K.-W.; Pan, S.-Y.; Chen, C.-T.; Chen, Y.-H.; Chiang, P.-C. High-gravity carbonation of basic oxygen furnace slag for CO_2 fixation and utilization in blended cement. *J. Clean. Prod.* **2016**, *124*, 350–360. [CrossRef]
255. Ghouleh, Z.; Guthrie, R.I.L.; Shao, Y. Production of carbonate aggregates using steel slag and carbon dioxide for carbon-negative concrete. *J. CO_2 Util.* **2017**, *18*, 125–138. [CrossRef]
256. Hobson, A.J.; Stewart, D.I.; Bray, A.W.; Mortimer, R.J.G.; Mayes, W.M.; Rogerson, M.; Burke, I.T. Mechanism of vanadium leaching during surface weathering of basic oxygen furnace steel slag blocks: A microfocus X-ray absorption spectroscopy and electron microscopy study. *Environ. Sci. Technol.* **2017**, *51*, 7823–7830. [CrossRef]
257. Yilmaz, D.; Lassabatere, L.; Deneele, D.; Angulo-Jaramillo, R.; Legret, M. Influence of carbonation on the microstructure and hydraulic properties of a basic oxygen furnace slag. *Vadose Zone J.* **2013**, *12*, 1–15. [CrossRef]
258. Yildirim, I.Z.; Prezzi, M. *Use of Steel Slag in Subgrade Applications*; Report FHWA/IN/JTRP-2009/32; Joint Transportation Research Program, Indiana Department of Transportation and Purdue University: West Lafayette, IN, USA, 2009. [CrossRef]
259. Teo, P.T.; Zakaria, S.K.; Salleh, S.Z.; Taib, M.A.A.; Sharif, N.M.; Seman, A.A.; Mohamed, J.J.; Yusoff, M.; Yusoff, A.H.; Mohamad, M.; et al. Assessment of electric arc furnace (EAF) steel slag waste's recycling options into value added green products: A review. *Metals* **2020**, *10*, 1347. [CrossRef]
260. Stroup-Gardiner, M.; Wattenberg-Komas, T. *Recycled Materials and Byproducts in Highway Applications Slag Byproducts, Volume 5: Slag Byproducts*; Transportation Research Board: Washington, DC, USA, 2013.
261. Bonvin, D. X-ray fluorescence spectrometry in the iron and steel industry. In *Encyclopedia of Analytical Chemistry*; Meyers, R.A., Ed.; Wiley: Hoboken, NJ, USA, 2000; pp. 9009–9028.
262. Lu, L.; Ward, M.; McLean, A. Chemical analysis of powdered metallurgical slags by X-ray fluorescence spectrometry. *ISIJ Int.* **2003**, *43*, 1940–1946. [CrossRef]
263. Aimoto, M.; Kanehashi, K.; Fujioka, Y. Analytical technologies for steel slags. *Nippon Steel Tech. Rep.* **2015**, *109*, 16–22.
264. Waligora, J.; Bulteel, D.; Degrugilliers, P.; Damidot, D.; Potdevin, J.L.; Measson, M. Chemical and mineralogical characterizations of LD converter steel slags: A multi-analytical techniques approach. *Mater. Charact.* **2010**, *61*, 39–48. [CrossRef]
265. Farrell, R.F.; Mackie, A.J.; Lessick, W.R. *Analysis of Steelmaking Slags by Atomic Absorption Spectrophotometry Using Pressure Dissolution*; United States Bureau of Mines: Washington, DC, USA, 1979.
266. Yildirim, I.Z.; Prezzi, M. Chemical, mineralogical, and morphological properties of steel slag. *Adv. Civ. Eng.* **2011**, *2011*, 463638. [CrossRef]
267. Nicolae, M.; Vîlciu, I.; Zăman, F. X-ray diffraction analysis of steel slag and blast furnace slag viewing their use for road construction. *UPB Sci. Bull. Ser. B Chem. Mater. Sci.* **2007**, *69*, 99–108.
268. König, U.; Gobbo, L.; Reiss, C. Quantitative XRD for ore, sinter, and slag characterization in the steel industry. In *Proceedings of the 10th International Congress for Applied Mineralogy*; Broekmans, M.A.T.M., Ed.; Springer: Berlin/Heidelberg, Germany, 2012; pp. 385–393.
269. Mos, Y.M.; Vermeulen, A.C.; Buisman, C.J.N.; Weijma, J. X-ray diffraction of iron containing samples: The importance of a suitable configuration. *Geomicrobiol. J.* **2018**, *35*, 511–517. [CrossRef]
270. Bunaciu, A.A.; Udriştioiu, E.G.; Aboul-Enein, H.Y. X-Ray diffraction: Instrumentation and applications. *Crit. Rev. Anal. Chem.* **2015**, *45*, 289–299. [CrossRef]
271. Holder, C.F.; Schaak, R.E. Tutorial on powder X-ray diffraction for characterizing nanoscale materials. *ACS Nano* **2019**, *13*, 7359–7365. [CrossRef]
272. Madsen, I.C.; Scarlett, N.V.Y.; Cranswick, L.M.D.; Lwin, T. Outcomes of the International Union of Crystallography Commission on Powder Diffraction Round Robin on Quantitative Phase Analysis: Samples 1a to 1h. *J. Appl. Crystallogr.* **2001**, *34*, 409–426. [CrossRef]
273. Fransen, M.J. 1- and 2-dimensional detection systems and the problem of sample fluorescence in X-ray diffractometry. *Adv. X-ray Anal.* **2004**, *47*, 224–231. [CrossRef]

274. Vaverka, J.; Sakurai, K. Quantitative determination of free lime amount in steelmaking slag by X-ray diffraction. *ISIJ Int.* **2014**, *54*, 1334–1337. [CrossRef]
275. De la Torre, A.G.; Bruque, S.; Aranda, M.A.G. Rietveld quantitative amorphous content analysis. *J. Appl. Crystallogr.* **2001**, *34*, 196–202. [CrossRef]
276. ASTM STP985. *Rapid Methods for Chemical Analysis of Hydraulic Cement*; Gebhardt, R.F., Ed.; American Society for Testing and Materials: West Conshohocken, PA, USA, 1988.
277. Javellana, M.P.; Jawed, I. Extraction of free lime in portland cement and clinker by ethylene glycol. *Cem. Concr. Res.* **1982**, *12*, 399–403. [CrossRef]
278. MacPherson, D.R.; Forbrich, L.R. Determination of uncombined lime in portland cement: The ethylene glycol method. *Ind. Eng. Chem. Anal. Ed.* **1937**, *9*, 451–453. [CrossRef]
279. Brand, A.S.; Roesler, J.R. Expansive and concrete properties of SFS–FRAP aggregates. *J. Mater. Civ. Eng.* **2016**, *28*, 1–10. [CrossRef]
280. Kneller, W.A.; Gupta, J.; Borkowski, M.L.; Dollimore, D. Determination of original free lime content of weathered iron and steel slags by thermogravimetric analysis. *Transp. Res. Rec.* **1994**, *1434*, 17–22.
281. Gumieri, A.G.; Dal Molin, D.C.C.; Vilela, A.C.F. Characteristics of steel slag granulated in a steel plant—Valuation of the microstructure through electron probe micro analysis. In *International RILEM Conference on the Use of Recycled Materials in Building and Structures, 2004*; Vázquez, E., Hendriks, C.F., Janssen, G.M.T., Eds.; RILEM: Paris, France, 2004; Volume 2, pp. 1067–1075. [CrossRef]
282. Lun, Y.; Zhou, M.; Cai, X.; Xu, F. Methods for improving volume stability of steel slag as fine aggregate. *J. Wuhan Univ. Technol. Sci. Ed.* **2008**, *23*, 737–742. [CrossRef]
283. Lee, H.-S.; Lim, H.-S.; Ismail, M.A. Quantitative evaluation of free CaO in electric furnace slag using the ethylene glycol method. *Constr. Build. Mater.* **2017**, *131*, 676–681. [CrossRef]
284. Goto, H.; Kakita, Y. Determination of free lime in slag. *Sci. Rep. Res. Inst. Tohoku Univ. Ser. A Phys. Chem. Metall.* **1955**, *7*, 135–139.
285. Chandru, P.; Karthikeyan, J.; Natarajan, C. Steel slag—A strong and sustainable substitute for conventional concreting materials. In *Sustainable Materials in Building Construction*; Delgado, J., Ed.; Springer: Cham, Switzerland, 2020; pp. 31–76.
286. Inoue, R.; Suito, H. Hydration of crystallized lime in BOF slags. *ISIJ Int.* **1995**, *35*, 272–279. [CrossRef]
287. Juckes, L.M. *Improved Utilisation of Blast Furnace and Steel Works Slags*; Report EUR 11681 EN; Commission of the European Communities: Luxembourg, 1996.
288. Arjunan, P.; Kumar, A. Rapid techniques for determination of free lime and free magnesia in cement clinker and portlandite in hydrates. *Cem. Concr. Res.* **1994**, *24*, 343–352. [CrossRef]
289. Hanada, K.; Inose, M.; Sato, S.; Watanabe, K.; Fujimoto, K. Development of analytical methods for free-MgO in steelmaking slag. *Tetsu-to-Hagane* **2016**, *102*, 24–28. [CrossRef]
290. Uehara, N.; Takita, M. Extraction of free magnesia from steelmaking slags using iodine–ethanol solutions. *ISIJ Int.* **2018**, *58*, 1474–1479. [CrossRef]
291. Kanehashi, K.; Aimoto, M. A new approach to quantification of free MgO in steelmaking slag by using solid-state ^{25}Mg NMR spectroscopy. *Tetsu-to-Hagane* **2013**, *99*, 543–551. [CrossRef]
292. Goldring, D.C.; Juckes, L.M. Petrology and stability of steel slags. *Ironmak. Steelmak.* **1997**, *24*, 447–456.
293. Kato, M.; Tsukagoshi, K.; Aimoto, M.; Saito, S.; Shibukawa, M. Determination of free magnesium oxide in steelmaking slags by microwave-assisted-hydration/thermogravimetry. *ISIJ Int.* **2018**, *58*, 1834–1839. [CrossRef]
294. Juckes, L.M. The volume stability of modern steelmaking slags. *Miner. Process. Extr. Metall.* **2003**, *112*, 177–197. [CrossRef]
295. Crawford, C.B.; Burn, K.N. Building damage from expansive steel slag backfill. *J. Soil Mech. Found. Div.* **1969**, *95*, 1325–1334.
296. Armaghani, J.M.; Larsen, T.J.; Smith, L.L. Design related distress in concrete pavements. *Concr. Int.* **1988**, *10*, 43–49.
297. Gnaedinger, J.P. Open hearth slag—A problem waiting to happen. *J. Perform. Constr. Facil.* **1987**, *1*, 78–83. [CrossRef]
298. Morales, E.M. Structural and functional distress due to slag expansion. In Proceedings of the Third International Conference on Case Histories in Geotechnical Engineering, St. Louis, MO, USA, 31 May–6 June 1993; Prakash, S., Ed.; University of Missouri-Rolla: Rolla, MO, USA, 1993; pp. 1139–1152.

299. Uppot, J.O. Structural fill of steel slag caused heave of a building. In Proceedings of the First International Conference on Case Histories in Geotechnical Engineering, St. Louis, MO, USA, 6 May 1984; Prakash, S., Ed.; University of Missouri-Rolla: Rolla, MO, USA, 1984; pp. 295–297.
300. Fronek, B.; Bosela, P.; Delatte, N. Steel slag aggregate used in portland cement concrete: U.S. and international perspectives. *Transp. Res. Rec.* **2012**, *2267*, 37–42. [CrossRef]
301. Howard, I.L.; Zimber, T.; Cook, K.; Yzenas, J.J., Jr.; Cagle, T.; Ayers, L.E.W. *Steel Slag as a Paving Aggregate: Properties, Applications, and Comparison to Alternatives*; Report No. CMRC WS 19-1; Mississippi State University: Starkville, MS, USA, 2019.
302. Okamoto, A.; Futamura, E.; Kawamura, K. Hydration behavior of LD slag at autoclave test. *Trans. Iron Steel Inst. Jpn.* **1981**, *21*, 16–24. [CrossRef]
303. Wang, Q.; Shi, M.; Zhang, Z. Hydration properties of steel slag under autoclaved condition. *J. Therm. Anal. Calorim.* **2015**, *120*, 1241–1248. [CrossRef]
304. Kuo, W.-T.; Shu, C.-Y. Effect of particle size and curing temperature on expansion reaction in electric arc furnace oxidizing slag aggregate concrete. *Constr. Build. Mater.* **2015**, *94*, 488–493. [CrossRef]
305. Deniz, D.; Tutumluer, E.; Popovics, J.S. Evaluation of expansive characteristics of reclaimed asphalt pavement and virgin aggregate used as base materials. *Transp. Res. Rec.* **2010**, *2167*, 10–17. [CrossRef]
306. Wang, G.; Wang, Y.; Gao, Z. Use of steel slag as a granular material: Volume expansion prediction and usability criteria. *J. Hazard. Mater.* **2010**, *184*, 555–560. [CrossRef]
307. Rohde, L.; Peres Núñez, W.; Augusto Pereira Ceratti, J. Electric arc furnace steel slag: Base material for low-volume roads. *Transp. Res. Rec.* **2003**, *1819*, 201–207. [CrossRef]
308. Dayioglu, A.Y.; Aydilek, A.H.; Cetin, B. Preventing swelling and decreasing alkalinity of steel slags used in highway infrastructures. *Transp. Res. Rec.* **2014**, *2401*, 52–57. [CrossRef]
309. Verhasselt, A.; Choquet, F. Steel slags as unbound aggregate in road construction: Problems and recommendations. In *Unbound Aggregates in Roads*; Jones, R.H., Dawson, A.R., Eds.; Butterworths: London, UK, 1989; pp. 204–211.
310. Yildirim, I.Z.; Prezzi, M. Geotechnical properties of fresh and aged basic oxygen furnace steel slag. *J. Mater. Civ. Eng.* **2015**, *27*, 4015046. [CrossRef]
311. Horii, K.; Tsutsumi, N.; Kitano, Y.; Kato, T. Processing and reusing technologies for steelmaking slags. *Nippon Steel Tech. Rep.* **2013**, *104*, 123–129.
312. Kumar, P.; Kumar, D.S.; Marutiram, K.; Prasad, S.M.R. Pilot-scale steam aging of steel slags. *Waste Manag. Res.* **2017**, *35*, 602–609. [CrossRef] [PubMed]
313. Herbelin, M.; Bascou, J.; Lavastre, V.; Guillaume, D.; Benbakkar, M.; Peuble, S.; Baron, J.-P. Steel slag characterisation—Benefit of coupling chemical, mineralogical and magnetic techniques. *Minerals* **2020**, *10*, 705. [CrossRef]
314. Riboldi, A.; Borgese, L.; Vassalini, I.; Cornacchia, G.; Gelfi, M.; Boniardi, M.V.; Casaroli, A.; Depero, L.E. Micro-Raman spectroscopy investigation of crystalline phases in EAF slag. *Appl. Sci.* **2020**, *10*, 4115. [CrossRef]
315. Mombelli, D.; Mapelli, C.; Barella, S.; Di Cecca, C.; Le Saout, G.; Garcia-Diaz, E. The effect of microstructure on the leaching behaviour of electric arc furnace (EAF) carbon steel slag. *Process Saf. Environ. Prot.* **2016**, *102*, 810–821. [CrossRef]